Design, Synthesis and Biological Evaluation of 3-(Imidazo[1,2-*a*]pyrazin-3-ylethynyl)-4-isopropyl-*N*-(3-((4-methylpiperazin-1-yl)methyl)-5-(trifluoromethyl)phenyl)benzamide as Dual Inhibitors of Discoidin Domain Receptor 1 and 2 (DDR1/2)

Zhen Wang,[†,ε,#] *Yali Zhang,*[§,#] *Daniel M. Pinkas,*[Φ,#] *Alice E. Fox*[Φ], *JinfengLuo,*[ε] *HuocongHuang,*[&] *Shengyang Cui,*[ε] *Qiuping Xiang,*[ε] *TingtingXu,*[Ψ] *QiujuXun,*[ε] *Dongsheng Zhu,*[ε] *ZhengchaoTu,*[ε] *XiaomeiRen,*[†] *Rolf A. Brekken,*[&] *Alex N. Bullock,*[Φ] *Guang Liang,*[§,*] *Ke Ding,*[†,*] *Xiaoyun Lu*[†,*]

[†]International Cooperative Laboratory of Traditional Chinese Medicine Modernization and Innovative Drug Development of Chinese Ministry of Education (MOE), Guangzhou City Key Laboratory of Precision Chemical Drug Development, School of Pharmacy, Jinan University, 601 Huangpu Avenue West, Guangzhou 510632, China

[ε] Guangzhou Institutes of Biomedicine and Health, Chinese Academy of Sciences, 190 Kaiyuan Avenue, Guangzhou 510530, China

[§]Chemical Biology Research Centre, School of Pharmaceutical Sciences, Wenzhou Medical University, Wenzhou325035, China

[Ψ]Department of Pulmonary Medicine, the 2nd affiliated hospital, Wenzhou Medical University, Wenzhou325035, China

[&]Nancy B. and Jake L. Hamon Centre for Therapeutic Oncology Research, Departments of Surgery and Pharmacology, UT Southwestern Medical Centre at Dallas, 5323 Harry Hines Blvd.Dallas, TX75390, USA

[Φ]Structural Genomics Consortium, University of Oxford, Old Road Campus Research Building, Roosevelt Drive, Oxford OX3 7DQ, UK

Key Words: DDR1, DDR2, dual inhibitor, anti-inflammation, acute lung injury (ALI)

ABSTRACT: Discoidin domain receptor 1 and 2 (DDR1 and DDR2) are new potential targets for anti-inflammatory drug discovery. A series of heterocycloalkynylbenzimides were designed and optimized to co-inhibit DDR1 and DDR2. One of the most promising compounds, **5n**, tightly bound to DDR1 and DDR2 protein with K_d values of 7.9 and 8.0 nM, and potently inhibited the kinases with IC_{50} values of 9.4 and 20.4 nM, respectively, while was significantly less potent for a panel of 403 wild-type kinases at 1.0 μM. DDR1 and DDR2 kinase inhibition by **5n** was validated by Western blotting analysis in primary human lung fibroblasts. The compound also dose-dependently inhibited lipopolysaccharide (LPS)-induced interleukin-6 (IL-6) release *in vitro*, and exhibited promising *in vivo* anti-inflammatory effect in a LPS-induced acute lung injury (ALI) mouse model. Compound **5n** may serve as a lead compound for new anti-inflammatory drug discovery.

INTRODUCTION

Discoidin domain receptors (DDRs), including DDR1 and DDR2, are non-integrin collagen receptor kinases with a unique extracellular domain homologous to discoidin I protein of Dictyostelium discoideum.[1-7] DDRs are involved in the regulation of cellular morphogenesis, differentiation, proliferation, adhesion, migration, and invasion.[1-7] Collective evidence demonstrates that DDR1 and DDR2 are critical mediators of inflammatory cytokine secretion.[2,4,7] Dysregulation of the receptors has been implicated in a variety of inflammatory diseases, such as atherosclerosis, osteoarthritis, and organ fibrosis.[1-7] For instance, collagen induced activation of DDR1b markedly amplifies the production of interleukin-8 (IL-8), macrophage inflammatory protein-1α (MIP-1α), and monocyte chemoattractant protein-1 (MCP-1) by macrophages during inflammatory responses.[8] Renal cortical slices of DDR1 null mice showed a blunted response of chemokine secretion to lipopolysaccharide (LPS) that was accompanied by protection against LPS-induced mortality.[9] A similar situation was also found in bleomycin-induced lung injury.[10] Pharmacological inhibition of DDR1 by small molecules has been shown to reduce inflammatory cytokines and demonstrate promising therapeutic effects in mouse inflammation models.[11,12] Activation of DDR2 was also reported to increase the production of cytokines such as IL-12, tumor necrosis factor-α (TNF-α), and interferon-γ (INF-γ) by human dendritic cells,[13,14] and contribute significantly to inflammatory disorders. Collagen I mediated activation of DDR2 is critical for fibrogenesis and promotes resolution of lung inflammation.[15] Silencing DDR2 expression was reported to decrease alcohol-induced liver injury and fibrosis in a model for early stage alcoholic liver disease.[16] Additionally, DDR2 can mediate hepatic stellate cell activation, proliferation and migration during acute liver injury, highlighting the profibrotic activity of DDR2.[17] Other studies also reported that activation of DDR2 by collagen I could induce the expression of DDR1 in primary human lung fibroblasts,[18]

indicating potential crosstalk between these two receptors. Therefore, dual inhibition of DDR1 and DDR2 might be a promising strategy for anti-inflammatory drug discovery.

A number of DDR1 and DDR2 inhibitors have been reported to date (Figure **1**). However, most of these molecules suffer from relatively low target specificity.[19-21] For example, In addition to DDR1/2, inhibitors **1** and **2** also show strong inhibition against Abl, c-Kit, and cSrc. 4-[(4-Methylpiperazin-1-yl)methyl]-*N*-(4-methyl-3-{[4-(pyridin-3-yl)pyrimidin-2-yl]amino}phenyl)benzamide (imatinib), 4-methyl-*N*-[3-(4-methyl-1*H*-imidazol-1-yl)-5-(trifluoro-methyl)phenyl]-3-[(4-pyridin-3-ylpyrimidin-2-yl)amino]benzamide (nilotinib), *N*-(2-chloro-6-methylphenyl)-2-[[6-[4-(2-hydroxyethyl)-1-piperazinyl]-2-methyl-4-pyrimidinyl]amino]-5-thiazolecarboxamide (dasatinib) exhibit strong DDR1/2 inhibitory activities, but neither DDR1 nor DDR2 is their primary target.[22] It is highly desirable to identify new selective DDR1/2 dual inhibitors for biological investigation and therapeutic development. Herein, we report the design and synthesis of heterocycloalkynylbenzimides as new selective DDR1/2 dual inhibitors with promising *in vivo* therapeutic effect in a LPS-induced acute lung injury (ALI) mouse model.

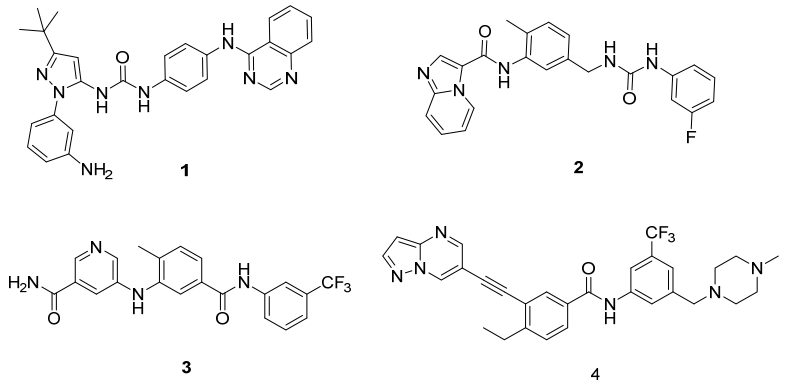

Figure 1. Chemical structures of the representative reported DDR1/2 inhibitors.

CHEMISTRY

The designed DDR1/2 inhibitors were readily prepared using palladium-catalyzed Sonogashira coupling[23] as the key steps (Scheme 1). Briefly, commercially available methyl 3-aminobenzoates (**6**) went through diazotization and iodization to yield intermediates **7**, which were treated with ethynyltrimethylsilane under palladium catalysis to afford the Sonogashira coupling products, deprotection of which produced the terminal alkynes (**8**). Intermediates **8** were reacted with 3-((4-methylpiperazin-1-yl)methyl)-5-(trifluoromethyl)aniline to produce intermediate **9** under basic conditions. Compounds **9** coupled with aromatic bromides under Sonogashira conditions to give compounds **5a-5l**. Alternatively, intermediates **8** could also couple with aromatic bromides and then react with 3-((4-methylpiperazin-1-yl)methyl)-5-(trifluoromethyl)aniline under basic conditions to produce final products **5m-5r**.

Scheme 1. Synthesis of Compounds **5a-5r**.[a]

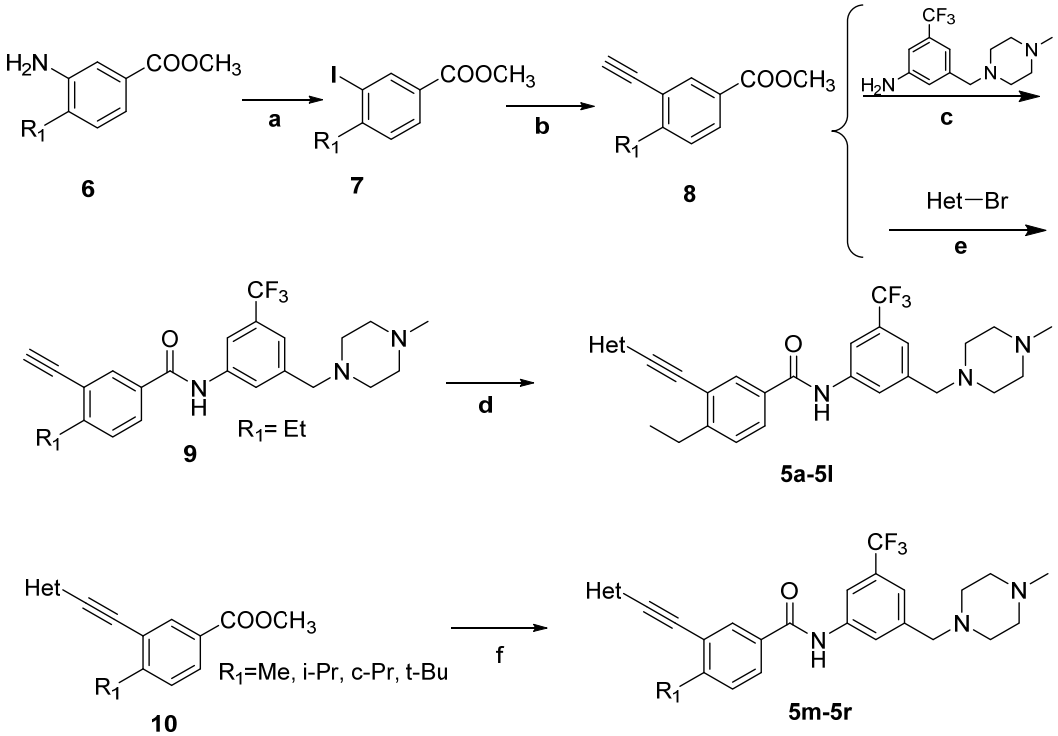

[a] **Reagents and conditions**: (a) i) conc. H_2SO_4, sodium nitrite ($NaNO_2$), H_2O; ii) potassium iodide (KI), H_2O, 40~70% (two steps); (b) i) trimethylsilyl acetylene, CuI, bis(triphenylphosphine)palladium (II) chloride ($PdCl_2(PPh_3)_2$), triethylamine (Et_3N), acetonitrile (MeCN), 60^oC; ii) K_2CO_3, MeOH, room temperature (rt), 88~92% (two steps); (c) t-BuOK, tetrahydrofuran (THF), -20 ^oC to rt, 92%; (d) Het-Br, CuI, $PdCl_2(PPh_3)_2$, ethyl diisopropylamine (DIPEA), *N, N*-dimethylformamide (DMF), 80 ^oC, 40~85%; (e) CuI, $PdCl_2(PPh_3)_2$, DIPEA, DMF, 80 ^oC, 64~91%; (f) 3-((4-methylpiperazin-1-yl)methyl)-5-(trifluoromethyl)aniline, t-BuOK, THF, -20 ^oC to rt, 74~87%.

MOLECULE DESIGN

Compound **4** (**7rh**) is a newly discovered selective DDR1 inhibitor from our group (Figure **2A**),[24] which potently inhibited the kinase activity of DDR1 with IC_{50} value of 9.7 nM. It also exhibited modest suppressive effect on DDR2 with an IC_{50} value of 175 nM, but was significantly less potent against the majority of a panel of 395 non-mutated kinases. In view of its promising target selectivity and outstanding pharmacokinetic (PK) properties,[24] compound **4** was chosen as a starting lead compound for further structural modification to achieve selective dual inhibition of DDR1 and DDR2.

DDR2 shares an approximate 57% sequence identity with DDR1 in its kinase domain (Figure S1).[7] Thus, a homologous model of DDR2 was first generated based on the DDR1 crystal structure (PDB code 3ZOS) to provide an initial structural basis for inhibitor optimization. It was shown that compound **4** could bind to the inactive configurations of DDR1 and DDR2 with similar type II binding modes (Figure 2A and 2B). The inhibitor was predicted to form four hydrogen bonds with the Met704, Glu672 and Asp784 residues of DDR1. Favorable van der Waals contacts could also be formed in the allosteric pocket. However, compound **4** failed to

form a hydrogen bond interaction with the corresponding Met95 of DDR2 due to the inappropriate orientation. Further investigation also suggested that the potential stereo hindrance between pyrazolo[1,5-a]pyrimidin head of **4** and the Tyr94 and Met95 hinge residues might contribute to significant less potency with DDR2 (Figure 2B). These preliminary computational analyses indicated that replacement of the pyrazolo[1,5-*a*]pyrimidine moiety with alternative hinge-binding heterocycles could be a feasible strategy to achieve dual inhibition against DDR1 and DDR2.

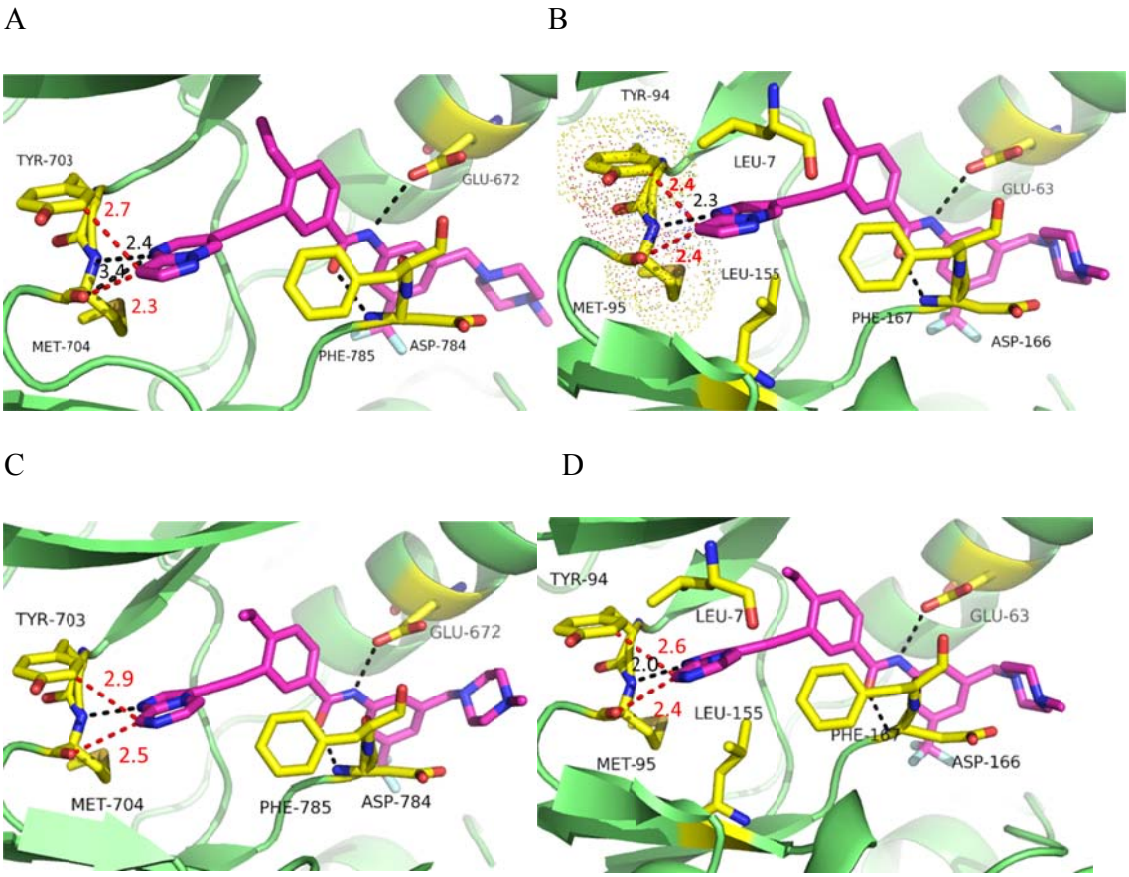

Figure 2. Potential binding modes of new inhibitors with DDR1 and DDR2 proteins. A) Molecular docking of **4** into DDR1 (PDB: 3ZOX); B) Molecular docking of **4** into the DDR2 homology model; C) Molecular docking of **5j** into the DDR1 structure (PDB: 3ZOX); D) Molecular docking of **5j** into DDR2 homology model. Regular hydrogen bonds are indicated by

black dashed lines. The distances between two atoms are indicated by red dashed line. The key residues are shown by yellow sticks.

RESULTS AND DISCUSSION

Compound **5a** with a pyrimidine moiety was first designed and synthesized to exhibit similar inhibitory potencies against DDR1 and DDR2 to that of inhibitor **4**. It was predicted that introduction of a hydrogen bond donating group at the 2-position of **5a** could potentially capture an additional hydrogen bond interaction with Met95 residue of DDR2 protein to improve its kinase inhibitory potency. Indeed, both the 2-aminopyrimidine (**5b**) and 2-(methylamino)pyrimidine (**5c**) derivatives displayed improved DDR2 inhibitory potencies with IC_{50} values of 45.3 and 83.1 nM, respectively (Table 1). The inhibitory activities against DDR1 were also improved by approximately 2 fold with IC_{50} values of 3.9 and 5.0 nM, respectively. Not surprisingly, when a dimethylamino group was introduced at the 2-position, the resulting compound (**5d**) almost totally abolished its inhibition of DDR1 and DDR2 kinases. Although compounds **5b** and **5c** exhibited good inhibitory potencies against DDR1 and DDR2, they were almost equally potent against Abl1. The lack of target specificity makes these compounds less attractive for further investigation. Several 5-member heterocycles were also utilized as the potential hinge binding moieties (Table 1). Although the introduction of 3-furan (**5e**), 3-thiophene (**5g**) or 2-furan (**5f**) significantly decreased the kinase inhibitory potencies against DDR1 and DDR2, the 1-methyl-*1H*-imidazole (**5h**) and 1, 2-dimethyl-*1H*-imidazole(**5i**) substituted derivatives exhibited strong inhibition against DDR1 and DDR2 kinases with IC_{50} values of 16.0, 7.9 and 94.2, 34.1 nM, respectively. Encouraged by the results of compounds **5h** and **5i**, bi-cyclic derivatives (**5j**, **5k**,and **5l**) were further designed and synthesized by utilizing a conformational constraint strategy.[25] It was shown the cyclization significantly improved their

potencies against both DDR1 and DDR2. Compounds **5j**, **5k**, and **5l** suppressed the kinase activity of DDR2 with IC_{50} values of 7.0, 13.1, and 10.4 nM, respectively. The compounds also displayed strong inhibition against DDR1 with IC_{50} values of 3.2, 3.9, and 6.2 nM, respectively. Thus, compound **5j** represented one of the most potent dual inhibitors against DDR1/DDR2 in these derivatives. Further computational study suggested that compound **5j** bound to DDR1 and DDR2 with a DFG-out conformation (Figure **2C** and **2D**). The imidazo[1,2-*a*]pyrazinegroup could fit nicely into the hinge region of DDR1 or DDR2 with a hydrogen bond interaction with Met704 or Met95, respectively (Figure **2D**). Unfortunately, compound **5j** also strongly inhibited the kinase activity of Abl1 with an IC_{50} value of 9.4 nM. Thus, further structural optimization was conducted with the aim to improve the inhibitor's target selectivity.

It has been previously demonstrated that the "flag methyl" group was critical for Abl1 inhibitors to achieve potency against the kinase.[26] Replacement of an original methyl with an ethyl group helped us to successfully identify a highly selective DDR1 inhibitor **4**.[24] It was hypothesized that the Abl1 inhibition might be diminished by optimizing the "flag ethyl" group in compound **5j**. Compounds **5m**, **5n**, **5o**, and **5p** were consequently designed and synthesized based on this hypothesis. It was shown that the "flag alkyl" moiety indeed had a significant impact on the inhibitory potency against Abl1. When the ethyl group in **5j** was replaced with a methyl substituent, the resulting compound **5m** demonstrated 24 fold improved potency against Abl1 with an IC_{50} value of 0.4 nM, but the modification barely affected the DDR1 and DDR2 inhibition. Encouragingly, the isopropyl derivative (**5n**) exhibited significantly decreased Abl1 inhibitory potency with an IC_{50} value of 494 nM, while it retained the strong inhibition against DDR1 and DDR2 with IC_{50} values of 9.4 and 20.4 nM, respectively. Compound **5n** represented one of the most selective DDR1/DDR2 dual inhibitors over Abl1. The cyclic propyl compound

5o was less selective, whereas the tert-butyl derivative **5p** almost totally abolished the DDR2 inhibition. The isopropyl group substituted compounds **5q** and **5r** also demonstrated obviously decreased Abl1 inhibition, but their potencies against DDR2 were also apparently lost. The relatively weak target inhibitory activities made compounds **5q** and **5r** less attractive for further biological investigation.

Table 1. *In Vitro* Inhibitory Activities of Compounds **5a-5r** against DDR1, DDR2, and Abl1[a,b]

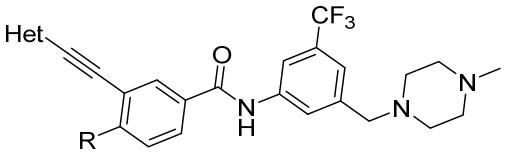

5

compd	Het	R	Kinase inhibition (IC_{50}, nM)		
			DDR1	DDR2	Abl1
4		Et	9.7±1.7	175±13	308±20
5a		Et	8.4± 0.4	221± 18	281 ± 12
5b	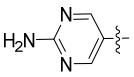	Et	3.9 ± 1.1	45.3 ± 2.7	21.0± 0.1
5c	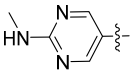	Et	5.0± 1.4	83.1 ± 4.2	30.2 ± 2.0
5d	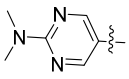	Et	614± 125	4800± 325	9700± 250

5e		Et	151±17	1540 ± 345	7700± 2300
5f		Et	1200± 230	2100± 302	>10000
5g		Et	695± 110	3800± 1000	>10000
5h		Et	16.0± 1.5	94.2± 4.2	346± 35
5i	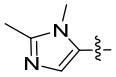	Et	7.9± 1.1	34.1± 2.9	97.4± 9.5
5j		Et	3.2± 0.3	7.0± 1.6	9.4± 0.1
5k		Et	3.9± 0.4	13.1± 0.6	11.9± 2.3
5l		Et	6.2± 1.0	10.4± 0.9	21.1± 2.6
5m	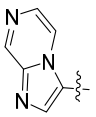	Me	2.4± 0.5	3.1± 0.5	0.4± 0.1
5n	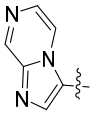	i-Pr	9.4± 0.9	20.4± 1.7	494± 64
5o		c-Pr	12.6± 1.3	40.2± 0.2	202± 11

5p		t-Bu	380 ±89	2200± 100	>10000
5q		i-Pr	11.4± 0.3	47.4± 3.8	564± 33
5r		i-Pr	12.5± 1.3	61.1± 3.3	932± 55

[a]DDR1 and DDR2 inhibition experiments were performed using the LANCE ULTRA kinase assay according to the manufacturer's instructions. [b]Abl1 activity experiments were performed using the FRET-based Z′-Lyte assay according to the manufacturer's instructions. The data are mean values from at least four independent experiments.

To elucidate the details of the interaction of **5n** with DDR1, we determined the X-ray co-crystal structure of their complex refined at 2.1Å resolution (Figure 3, Table S3). It was confirmed that **5n** fits nicely into the ATP binding site of DDR1 with a similar binding mode to that predicted by the docking model of **5j** (Figure 2C). The imidazo[1,2-*a*]pyrazine moiety of **5n** was observed to form an essential hydrogen bond with Met704 in the hinge region. Two additional hydrogen bonds were also formed between the amide and Glu672 and Asp784, respectively, while the flag isopropyl fitted nicely into a hydrophobic pocket formed by the residues Val624, Ala653, Lys655 and Met699.

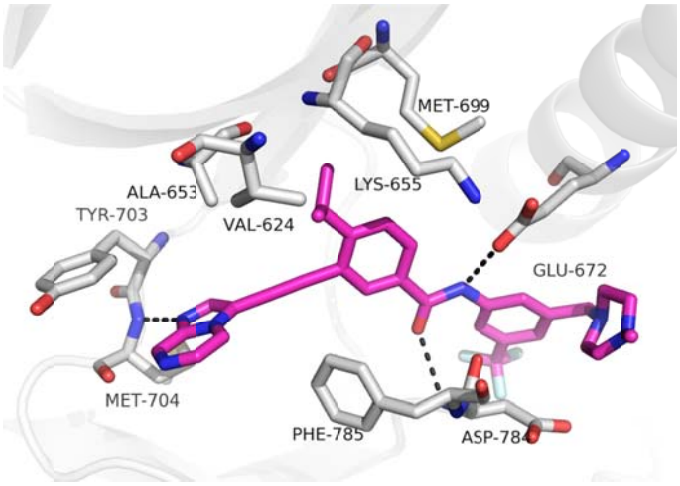

Figure 3. Co-crystal structure of **5n** with DDR1 (PDB ID: 6GWR). Hydrogen bonds are indicated by dashed black lines. The key residues are shown as gray sticks. Compound **5n** is shown as magenta sticks.

The DDR1/DDR2 dual inhibition by **5n** was validated by determining its binding affinities with the receptors (conducted by DiscoveRx, San Diego, CA).[27] It was shown that **5n** bound tightly to DDR1 and DDR2 with binding constant (K_d) values of 7.9 and 8.0 nM, respectively. The target selectivity of **5n** was further evaluated by conducting a kinase selectivity profiling study against a panel of 468 kinases (including 403 non-mutated kinases) at 1.0 μM, which is approximately 125 fold above its K_d values against the DDR1/2 targets. The results indicated that **5n** exhibited good target selectivity with S(10) and S(1) scores of 0.032 and 0.017, respectively (Supporting information).[27] For instance, **5n** showed 100% competition rate (100% inhibition, ctrl% = 0) with DDR1 and DDR2 at 1.0 μM, while it only showed obvious binding with a minor portion of the kinases investigated. The major "off target" (inhibition > 90%, ctrl% < 10) included Abl1, Ephrin type-A receptor 2 (EPHA2), EPHA7, EPHA8, Ephrin type-B receptor 2 (EPHB2), lymphocyte-specific protein tyrosine kinase (LCK), serine/threonine kinase 10 (LOK), angiopoietin-1 receptor (TIE2), nerve growth factor receptor A (TrkA), TrkB, and TrkC. The

binding affinities (K_d) or kinase inhibitory activities (IC_{50}) of compound **5n** against these "off targets" were further determined by using DiscoveRx's platform or our in-house kinase assays (Table **2**). It was shown that compound **5n** was approximately 10-46 fold less potent against the majority of the "off target" kinases. However, this compound seemed to be equally potent to human disease related LOK, TrkB, and TrkC.[28, 29] The off-target inhibition of **5n** on TrkB and TrkC was further proven by a LANCE ULTRA kinase assay, which exhibited IC_{50} values of 40 and 18 nM, respectively.

The inhibitory effect of compound **5n** on the activation of DDR1 and DDR2 was also investigated in primary human lung fibroblasts (Figure **4**). The results clearly revealed that **5n** dose-dependently inhibited the phosphorylation of DDR1 and DDR2, whereas it did not exhibit obvious impact on the activation of c-Abl at concentrations of 50 and 100 nM.

Table 2. Binding affinities of compound **5n** against a panel of "off target" kinases.

Kinase	K_d value or IC_{50} (nM)	Kinase	K_d value or IC_{50}(nM)
ABL1	494[b]	LOK	10[a]
EPHA2	260[a]	TIE2	370[a]
EPHA7	200[a]	TRKA	100[a]
EPHA8	79[a]	TRKB	11[a] (40)[b]
EPHB2	260[a]	TRKC	9.3[a] (18)[b]
LCK	180[a]	-	-

[a]The binding affinities (K_d) were determined by using DiscoveRx's platform. [b]The kinase inhibitory activities (IC_{50}) were evaluated by using "in-house" kinase assays. Reported data are means from two independent experiments.

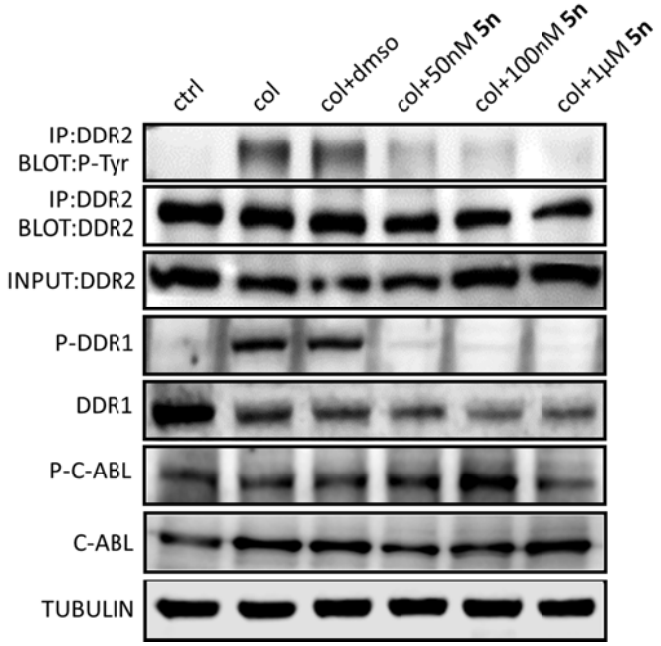

Figure 4. Effects of DDR1 and DDR2 inhibition on signaling by **5n** in primary human lung fibroblasts. Lysates were probed for the indicated targets by Western blot analysis. Primary human lung fibroblasts were treated with col I (50 μg/mL) and DMSO or different concentration of 5n for 8 hours. Cell lysates were harvested and subjected to immunoprecipitation or Western blot. Activation of DDR2 was detected by immunoprecipitation. Protein lysates were also probed for p-DDR1, DDR1, p-c-ABL, c-ABL and tubulin.

Given the critical function of DDR1 and DDR2 in the inflammatory process, we determined the potential anti-inflammatory effect of **5n** by measuring its capability to suppress the LPS-induced release of a representative cytokine, IL-6. It was shown that compound **5n** dose-dependently inhibited LPS-induced production of IL-6 in mouse primary peritoneal macrophages

(MPMs) as evaluated by using an enzyme linked immunosorbent assay (ELISA), supporting its promising *in vitro* anti-inflammatory activity (Figure **5).**

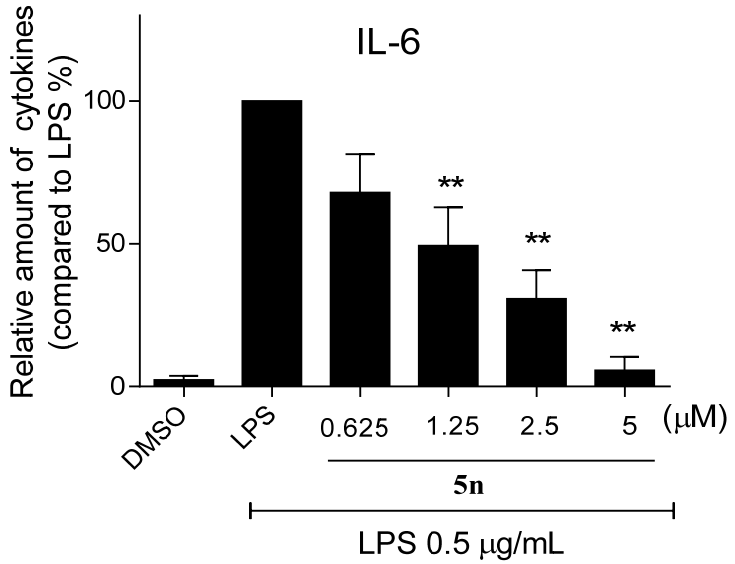

Figure 5. 5n inhibited LPS-induced IL-6 release in a dose-dependent manner in MPMs. Each bar represents mean ± SE of 3-5 independent experiments. Statistical significance relative to LPS is indicated, ** $p < 0.01$.

The potential therapeutic potential of **5n** was further investigated in a LPS-induced mouse acute lung injury (ALI) model.[30] Compound **5n** was orally administrated at 20 or 40 mg/kg twice daily (BID) for seven days prior to the administration of LPS (20 μL, 5 mg/kg) based on its pharmacokinetics parameters (Table S4). Pretreatment with compound **5n** reduced LPS-induced pulmonary edema as determined by lung Wet/Dry (W/D) ratio (Figure **6A**). The total protein concentrations in bronchial alveolar lavage fluid (BALF) were increased markedly after LPS administration compared to the control group (Figures **6B**), which was dose-dependently inhibited by **5n** (Figure **6B**). LPS instillation also resulted in significant pulmonary congestion, thickening of alveolar wall, and interstitial edema (Figure **6C**). These pathological changes

induced by LPS were significantly reduced by treatment with **5n** (Figure **6C**). Moreover, the compound was well tolerated and there was no animal death or obvious body weight change after the mice received 200 mg/kg or 400 mg/kg administration of compound **5n** (Supplemented Figure S3).

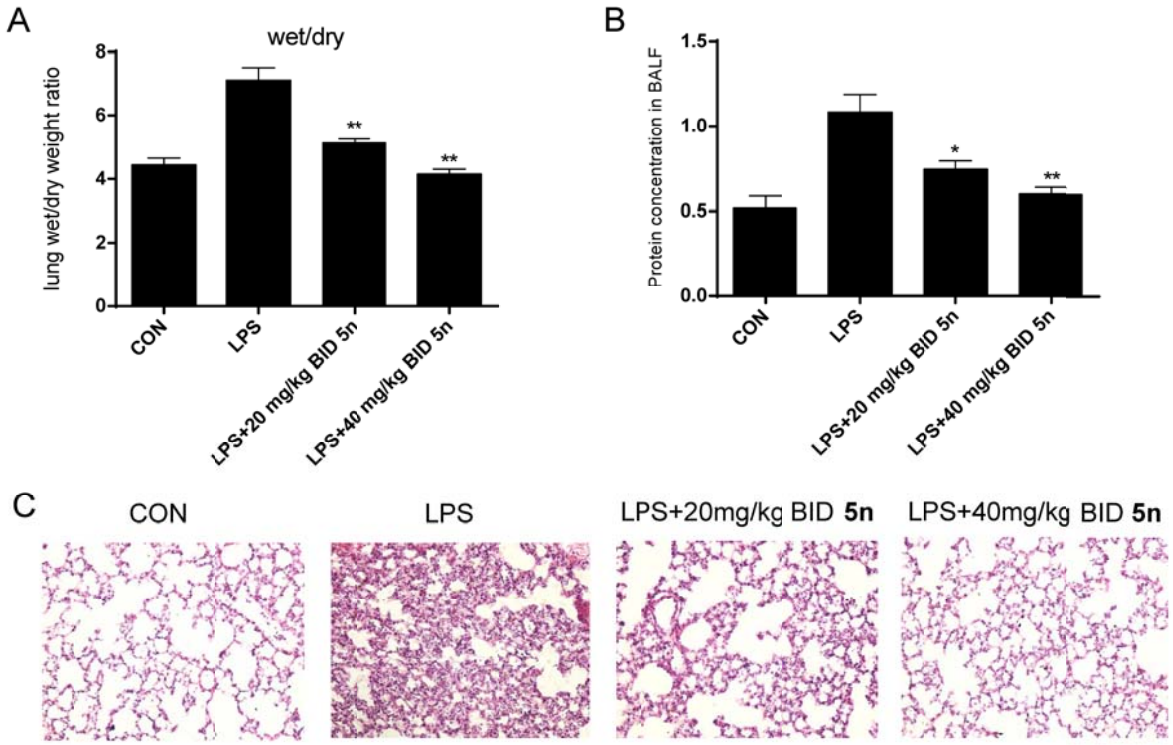

Figure **6**. Compound **5n** attenuated lung pathophysiologic changes in LPS-challenged mice. A) The lung W/D ratio. B) Protein concentration in BALF. C) H&E staining. Statistical significance relative to LPS group was indicated, * $p < 0.05$; ** $p < 0.01$.

Pro-inflammatory cytokines, which are secreted in the early phase of an inflammatory response, are critical in ALI. Thus, the levels of pro-inflammatory cytokines in BALF and serum were also determined. **5n** effectively decreased the levels of TNF-α and IL-6 both in BALF and serum (Figure **7A-D**). Additionally, LPS-induced elevation of neutrophils and total cell number

in BALF were also significantly reduced by treatment with **5n** (Figure **7E** and **7F**). We further examined the effect of **5n** on macrophage infiltration in lung tissue through CD68 immunohistochemical staining. As shown in Figure **7G**, LPS induced a significant accumulation of macrophages in the lung, whereas there was no significant difference in the number of CD68 positive macrophages between **5n**-treated and control groups. Thus, we concluded that administration of **5n** resulted in significant therapeutic protection from LPS-induced pulmonary inflammation *in vivo*.

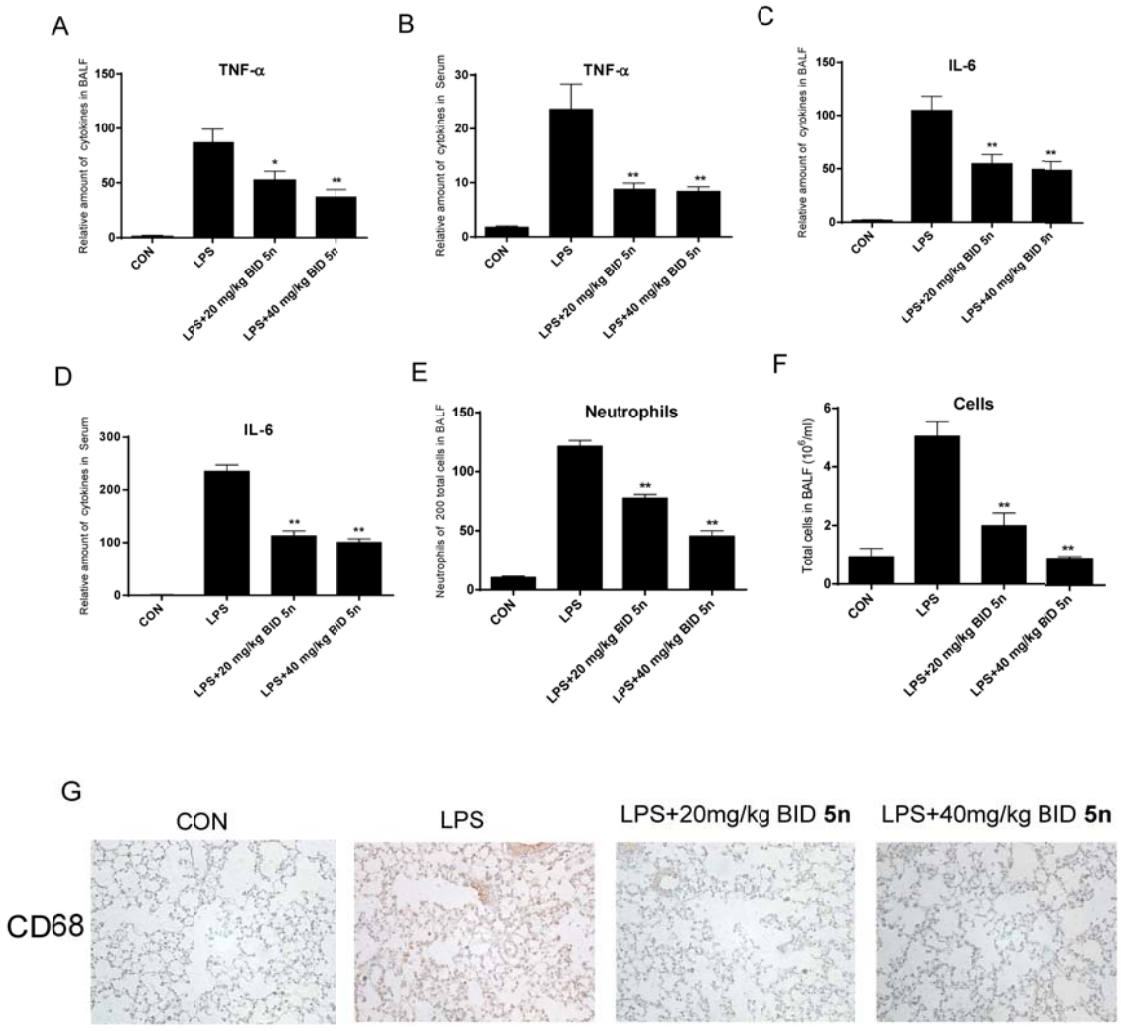

Figure **7**. **5n** attenuated lung inflammation in LPS-treated mice. A) The amount of cytokine TNF-α in BALF. B) The amount of cytokine TNF-α in serum. C) The amount of cytokine IL-6 in BALF. D) The amount of cytokine IL-6 in serum. E) The amount of neutrophils in BALF. F) The amount of total cells in BALF. G) Immunohistochemical of CD68 staining. Statistical significance relative to LPS group was indicated, *$p < 0.05$, **$p < 0.01$.

To confirm the anti-inflammatory effects of **5n**, we further evaluated the potency of the compound on inhibition of inflammatory gene expression. As shown in Figure **8**, LPS increased mRNA levels of pro-inflammatory cytokines TNF-α (**A**), IL-6 (**B**), IL-1β(**C**), IL-12 (**D**), and adhesion molecules intercellular cell adhesion molecule-1 (ICAM-1) (**E**), vascular cell adhesion molecule 1 (VCAM-1) (**F**), while compound **5n** treatment significantly abrogated LPS-induction of these inflammatory markers. The data collectively support that **5n** exhibits potent therapeutic effect on ALI by down-regulation of pro-inflammatory cytokine expression.

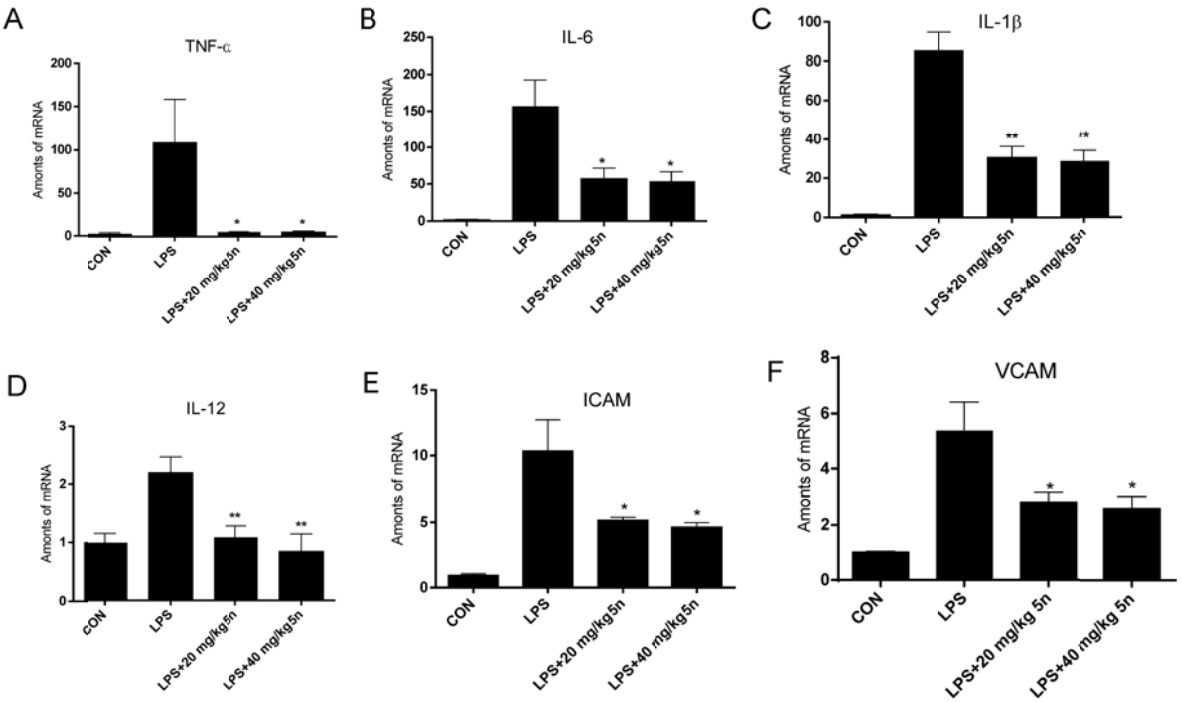

Figure **8**. Effects of **5n** on the expression of inflammatory genes in lung tissue. The levels of TNF-α (A), IL-6 (B), IL-1β (C), IL-12 (D), ICAM-1 (E), and VCAM-1 (F) were analyzed by RT-qPCR assay. Statistical significance relative to LPS group was indicated,*P < 0.05, **P < 0.01.

CONCLUSIONS

In summary, a series of heterocycloalkynylbenzimides were optimized to co-inhibit both DDR1 and DDR2. One of the most promising candidates **5n** tightly bound to the DDR1 and DDR2 proteins with K_d values of 7.9 and 8.0 nM, and potently inhibited DDR1 and DDR2 kinase function with IC_{50} values of 9.4 and 20.4 nM, respectively, while was obviously less potent against the majority of the 403 wild-type kinases at 1.0 μM. The compound exhibited promising anti-inflammatory effects *in vitro* and *in vivo*. To the best of our knowledge, this is the first *in vivo* investigation of selective DDR1/2 dual inhibitors as novel anti-inflammation agents.

EXPERIMENTAL SECTION

General Methods for Chemistry. All reagents and solvents were used as purchased from commercial sources without further purification. Flash chromatography was performed using 300 mesh silica gel. All reactions were monitored by TLC using silica gel plates with fluorescence F254 and UV light visualization. ^{1}H NMR spectra were recorded on a Bruker AV-400 spectrometer at 400 MHz or a Bruker AV-500 spectrometer at 500 MHz.^{13}C NMR spectra were recorded on a Bruker AV-500 spectrometer at 125 MHz. Coupling constants (*J*) are expressed in hertz (Hz). Chemical shifts (δ) of NMR are reported in parts permillion (ppm) units relative to an internal standard (TMS). The low or high resolution of ESI-MS was recorded on an Agilent 1200 HPLC-MSD mass spectrometer or Applied Biosystems Q-STAR Elite ESI-LC-

MS/MS mass spectrometer, respectively. Purity of the final compounds **5a**–**5r** was determined by reverse-phase high performance liquid chromatography [HPLC, Dionex Summit HPLC (Column: Diamonsil C18, 5.0 μm, 4.6 × 250 mm (Dikma Technologies); detector: PDA-100 photodiode array; injector: ASI-100 autoinjector; pump: p-680A)] to be >95%. A flow rate of 1.0 mL/min was used with mobile phase of 90%MeOH in H_2O with 0.1% modifier (ammonia, v/v).

4-Ethyl-*N*-(3-((4-methylpiperazin-1-yl)methyl)-5-(trifluoromethyl)phenyl)-3-(pyrimidin-5-ylethynyl)benzamide (5a).To a solution of 4-ethyl-3-ethynyl-*N*-(3-((4-methylpiperazin-1-yl)methyl)-5-(trifluoromethyl)phenyl)benzamide (487 mg, 1.13 mmol) in DMF (10 mL) was added 5-bromopyrimidine (200 mg, 1.26 mmol), DIPEA (0.4 ml, 2.26 mmol), $PdCl_2(PPh_3)_2$ (80 mg, 0.11 mmol), and CuI (21 mg, 0.11 mmol). The mixture was filled with Ar and stirred at 80 ^oC overnight. The mixture was poured into ice-water and the precipitate was collected and further purified by flash chromatography on silica gel to give the final compound **5a** (464 mg, 81% yield). ^1H NMR(400 MHz, DMSO-d_6) δ 10.59 (s, 1 H), 9.23 (s, 1 H), 9.07 (s, 2 H), 8.22 (d, J = 1.6 Hz, 1 H), 8.19 (s, 1 H), 8.02 (s, 1 H), 8.01 (dd, J = 8.0, 1.6 Hz, 1 H), 8.00 (d, J = 1.6 Hz, 1 H), 7.56 (d, J = 8 Hz, 1 H), 7.35 (s, 1 H), 3.54 (s, 2 H), 2.94 (q, J = 7.6 Hz, 2 H), 2.39 (br s, 4 H), 2.34 (br s, 4 H), 2.15 (s, 3 H), 1.28 (t, J = 7.6 Hz, 3 H). ^{13}C NMR (125 MHz, DMSO-d_6) δ165.1, 159.0, 157.4, 150.3, 141.2, 140.3, 132.7, 131.7, 129.7, 129.6 (q, J = 31.1 Hz), 129.0, 124.6 (q, J = 270.8 Hz), 124.2, 120.9, 120.4, 119.2, 115.5(d, J = 3.6 Hz), 93.8, 87.2, 61.8, 55.1, 52.9, 46.1, 27.5, 14.9. HRMS (ESI) for $C_{28}H_{28}F_3N_5O$ $[M + H]^+$, calcd: 508.2319, Found: 508.2316. Purity 99.5% (t_R = 12.79 min).

3-((2-Aminopyrimidin-5-yl)ethynyl)-4-ethyl-*N*-(3-((4-methylpiperazin-1-yl)methyl)-5-(trifluoromethyl)phenyl)benzamide (5b). Compound **5b** was prepared by following a similar procedure as that of**5a**. Yield, 70%. ^1H NMR(400 MHz, DMSO-d_6) δ 10.53 (s, 1 H), 8.47 (s, 2

H), 8.19(s, 1 H), 8.12 (s, 1H), 8.01 (s, 1 H), 7.92 (d, *J* = 8.0 Hz, 1 H), 7.49 (d, *J* = 8.0 Hz, 1 H), 7.35 (s, 1 H), 7.19 (s, 2 H), 3.54(s, 2 H), 2.89 (q, *J* = 7.2 Hz, 2 H), 2.40 (br s, 4 H), 2.33 (br s, 4 H), 2.15 (s, 3 H), 1.26 (t, *J* = 7.2 Hz, 3 H). ^{13}C NMR (125 MHz, DMSO-d_6) δ 165.3, 162.5, 160.6, 149.5, 141.2, 140.4, 132.6, 131.0, 129.7 (q, *J* = 30.6 Hz), 128.8, 128.5, 124.6 (q, *J* = 271.5 Hz), 124.2, 122.3, 120.4, 115.5, 106.3, 90.1, 89.5, 61.9, 55.1, 53.0, 46.1, 27.5, 14.9. HRMS (ESI) for $C_{28}H_{29}F_3N_6O$ $[M + H]^+$, calcd: 523.2428, Found: 523.2414. Purity 99.6% (t_R = 12.05 min).

4-Ethyl-3-((2-(methylamino)pyrimidin-5-yl)ethynyl)-*N*-(3-((4-methylpiperazin-1-yl)methyl)-5-(trifluoromethyl)phenyl)benzamide (5c*).* Compound **5c** was prepared by following a similar procedure as that of**5a**. Yield, 76%.^{1}H NMR(400 MHz, DMSO-d_6) δ 10.53 (s, 1 H), 8.53-8.48 (m, 2 H), 8.19 (s, 1 H), 8.12 (s, 1 H), 8.02 (s, 1 H), 7.93-7.91 (m, 1 H), 7.65-7.64 (m, 1 H), 7.50 (d, *J* = 8.0 Hz, 1 H), 7.35 (s, 1 H), 3.54 (s, 2 H), 2.90 (q, *J* = 7.6 Hz, 2 H), 2.85 (d, *J* = 4.8 Hz, 3 H), 2.40 (br s, 4 H), 2.34 (br s, 4 H), 2.15 (s, 3 H), 1.26 (t, *J* = 7.6 Hz, 3 H). ^{13}C NMR (125 MHz, DMSO-d_6) δ 165.3, 161.5, 160.4, 149.5, 141.1, 140.4, 132.6, 131.0, 129.7 (q, *J* = 31.4 Hz), 128.8, 128.5, 124.6 (q, *J* = 270.6 Hz), 124.2, 122.3, 120.4, 115.5, 105.8, 90.1, 89.6, 61.9, 55.1, 52.9, 46.1, 28.2, 27.5, 14.8. HRMS (ESI) for $C_{29}H_{31}F_3N_6O$ $[M + H]^+$, calcd: 537.2584, Found: 537.2584. Purity 98.7% (t_R = 14.44 min).

3-((2-(Dimethylamino)pyrimidin-5-yl)ethynyl)-4-ethyl-*N*-(3-((4-methylpiperazin-1-yl) methyl)-5-(trifluoromethyl)phenyl)benzamide (5d). Compound **5d** was prepared by following a similar procedure as that of **5a**. Yield, 77%. ^{1}H NMR (400 MHz, DMSO-d_6) δ 10.53 (s, 1 H), 8.56 (s, 2 H), 8.19 (s, 1 H), 8.13 (s, 1 H), 8.01 (s, 1 H), 7.92 (d, *J* = 8.0 Hz, 1 H), 7.49 (d, *J* = 8.0 Hz, 1 H), 7.35 (s, 1 H), 3.54 (s, 2 H), 3.17(s, 6 H), 2.89 (q, *J* = 7.2 Hz, 2 H), 2.40 (br s, 4 H), 2.33 (br s, 4 H), 2.15 (s, 3 H), 1.26 (t, *J* = 7.2 Hz, 3 H). ^{13}C NMR (125 MHz, DMSO-d_6) δ 165.2, 160.3, 160.1, 149.5, 141.1, 140.4, 132.6, 130.9, 129.6 (q, *J* = 31.1 Hz), 128.8, 128.5, 124.6 (q, *J*

= 270.8 Hz), 124.2, 122.2, 120.4, 115.5, 105.2, 90.3, 89.5, 61.9, 55.1, 52.9, 46.1, 37.1, 27.5, 14.8. HRMS (ESI) for $C_{30}H_{33}F_3N_6O$ $[M + H]^+$, calcd: 551.2741, Found: 551.2733. Purity 98.5% (t_R = 21.11 min).

4-Ethyl-3-(furan-3-ylethynyl)-*N*-(3-((4-methylpiperazin-1-yl)methyl)-5-(trifluoromethyl) phenyl)benzamide (5e). Compound **5e** was prepared by following a similar procedure as that of **5a**. Yield, 50%. ^{1}H NMR(400 MHz, DMSO-d_6) δ 10.53 (s, 1 H), 8.19-8.18 (m, 2 H), 8.13 (d, J = 1.6 Hz, 1 H), 8.01 (s, 1 H), 7.95-7.92 (m, 1 H), 7.81 (t, J = 1.6 Hz, 1 H), 7.50 (d, J = 8.0 Hz, 1 H), 7.35 (s, 1 H), 6.73 (d, J = 1.2 Hz, 1 H), 3.54(s, 2 H), 2.87 (q, J = 7.6 Hz, 2 H), 2.40 (br s, 4 H), 2.34 (br s, 4 H), 2.15 (s, 3 H), 1.26 (t, J = 7.6 Hz, 3 H). ^{13}C NMR (125 MHz, DMSO-d_6) δ 165.2, 149.6, 146.9, 144.5, 141.1, 140.4, 132.6, 131.1, 129.7 (q, J = 31.3 Hz), 128.8, 128.7, 124.6 (q, J = 270.7 Hz), 124.1, 122.1, 120.3, 115.5, 112.7, 89.1, 85.4, 61.9, 55.0, 52.9, 46.0, 27.5, 14.8. HRMS (ESI) for $C_{28}H_{28}F_3N_3O_2$ $[M + H]^+$, calcd: 496.2206, Found: 496.2204. Purity 98.6% (t_R = 14.21 min).

4-Ethyl-3-(furan-2-ylethynyl)-*N*-(3-((4-methylpiperazin-1-yl)methyl)-5-(trifluoromethyl)phenyl)benzamide (5f).Compound **5f** was prepared by following a similar procedure as that of **5a**. Yield, 46%. ^{1}H NMR(400 MHz, DMSO-d_6) δ 10.54 (s, 1 H), 8.18-8.17 (m, 2 H), 8.01 (s, 1 H), 7.98-7.96 (m, 1 H), 7.82 (d, J = 1.6 Hz, 1 H), 7.53 (d, J = 8.4 Hz, 1 H), 7.35 (s, 1 H), 6.96 (d, J = 3.6 Hz, 1 H), 6.65-6.64 (m, 1 H), 3.54(s, 2 H), 2.87 (q, J = 7.6 Hz, 2 H), 2.40 (br s, 4 H), 2.33 (br s, 4 H), 2.15 (s, 3 H), 1.26 (t, J = 7.6 Hz, 3 H). ^{13}C NMR (125 MHz, DMSO-d_6) δ 165.0, 149.7, 145.6, 141.1, 140.3, 136.1, 132.7, 131.1, 129.7 (q, J = 31.3 Hz), 129.3, 129.0, 124.6 (q, J = 270.8 Hz), 124.2, 121.0, 120.4, 116.7, 115.5, 112.1, 91.5, 83.8, 61.9, 55.0, 52.9, 46.1, 27.5, 14.8. HRMS (ESI) for $C_{28}H_{28}F_3N_3O_2$ $[M + H]^+$, calcd: 496.2206, Found: 496.2198. Purity 99.6% (t_R = 14.91 min).

4-Ethyl-*N*-(3-((4-methylpiperazin-1-yl)methyl)-5-(trifluoromethyl)phenyl)-3-(thiophen-3-ylethynyl)benzamide (5g). Compound **5g** was prepared by following a similar procedure as that of **5a**. Yield, 40%. ^{1}H NMR(400 MHz, DMSO-d_6) δ 10.54 (s, 1 H), 8.19 (s, 1 H), 8.15 (s, 1 H), 8.02 (s, 1 H), 7.94-7.93 (m, 2 H), 7.69-7.67 (m, 1 H), 7.50 (d, J = 8.0 Hz, 1 H), 7.35 (s, 1 H), 7.29 (d, J = 4.8 Hz, 1 H), 3.54(s, 2 H), 2.90 (q, J = 7.6 Hz, 2 H), 2.40 (br s, 4 H), 2.34 (br s, 4 H), 2.15 (s, 3 H), 1.27 (t, J = 7.2 Hz, 3 H). ^{13}C NMR (125 MHz, DMSO-d_6) δ 165.2, 149.8, 141.1, 140.4, 132.6, 131.2, 130.4, 129.9, 129.7 (q, J = 31.3 Hz), 128.7, 127.5, 124.6 (q, J = 270.6 Hz), 124.2, 122.1, 121.5, 120.3, 115.5, 89.4, 86.9, 61.9, 55.1, 52.9, 46.1, 27.6, 14.8. HRMS (ESI) for $C_{28}H_{28}F_3N_3OS$ $[M + H]^+$, calcd: 512.1978, Found: 512.1973. Purity 98.3% (t_R = 16.21 min).

***N*-(4-Ethyl-3-((1-methyl-*1H*-imidazol-5-yl)ethynyl)phenyl)-3-((4-methylpiperazin-1-yl) methyl)-5-(trifluoromethyl)benzamide (5h).** Compound **5h** was prepared by following a similar procedure as that of **5a**. Yield, 46%. ^{1}H NMR(400 MHz, DMSO-d_6) δ 10.54 (s, 1 H), 8.19 (s, 1 H), 8.16 (s, 1 H) 8.01 (s, 1 H), 7.95 (d, J = 8.0 Hz, 1 H), 7.82 (s, 1 H), 7.52 (d, J = 8.0 Hz, 1 H), 7.37 (s, 1 H), 7.35 (s, 1 H), 3.75 (s, 3 H), 3.54 (s, 2 H), 2.90 (q, J = 7.2 Hz, 2 H), 2.40 (br s, 4 H), 2.33 (br s, 4 H), 2.15 (s, 3 H), 1.27 (t, J = 7.6 Hz, 3 H). ^{13}C NMR (125 MHz, DMSO-d_6) δ 165.2, 149.4, 141.2, 140.3, 140.2, 134.6, 132.7, 130.9, 129.6 (q, J = 31.3 Hz), 128.9, 128.8, 124.6 (q, J = 270.7 Hz), 124.2, 121.7, 120.4, 115.5, 115.4, 94.2, 82.3, 61.8, 55.1, 52.9, 46.1, 32.2, 27.6, 14.9. HRMS (ESI) for $C_{28}H_{30}F_3N_5O$ $[M + H]^+$, calcd: 510.2475, Found: 510.2471. Purity 99.4% (t_R = 12.93 min).

***N*-(3-((1,2-dimethyl-*1H*-imidazol-5-yl)ethynyl)-4-ethylphenyl)-3-((4-methylpiperazin-1-yl) methyl)-5-(trifluoromethyl)benzamide (5i).**Compound **5i** was prepared by following a similar procedure as that of **5a**. Yield, 48%. ^{1}H NMR(400 MHz, DMSO-d_6) δ 10.5 (s, 1 H), 8.19 (s, 1 H), 8.15 (d, J = 1.2 Hz, 1 H), 8.01 (s, 1 H), 7.95-7.92 (m, 1 H), 7.51 (d, J = 8.4 Hz, 1 H), 7.35 (s, 1

H), 7.24 (s, 1 H), 3.64 (s, 3 H), 3.54 (s, 2 H), 2.89 (q, *J* = 7.6 Hz, 2 H), 2.40-2.36 (m, 11 H), 2.15 (s, 3 H), 1.27 (t, *J* = 7.6 Hz, 3 H). ^{13}C NMR (125 MHz, DMSO-d_6) δ 165.2, 149.1, 147.1, 141.1, 140.4, 133.0, 132.7, 130.8, 129.6 (q, *J* = 31.1Hz), 128.9, 128.7, 124.6 (q, *J* = 270.7 Hz), 124.2, 121.8, 120.3, 115.5, 115.3, 94.0, 83.1, 61.9, 55.1, 52.9, 46.1, 31.2, 27.6, 14.9, 13.6. HRMS (ESI) for $C_{29}H_{32}F_3N_5O$ $[M + H]^+$, calcd: 524.2632, Found: 524.2628. Purity 99.6% (t_R = 13.87 min).

4-Ethyl-3-(imidazo[1,2-*a*]pyrazin-3-ylethynyl)-*N*-(3-((4-methylpiperazin-1-yl)methyl)-5-(trifluoromethyl)phenyl)benzamide (5j). Compound **5j** was prepared by following a similar procedure as that of **5a**. Yield, 78%.^{1}H NMR(400 MHz, DMSO-d_6) δ 10.58 (s, 1 H), 9.21 (d, *J* = 1.6 Hz, 1 H), 8.64 (dd, *J* =4.8, 1.6 Hz, 1 H), 8.31 (d, *J* = 2.0 Hz, 1 H), 8.26 (s, 1 H), 8.19 (s, 1 H), 8.14 (d, *J* = 4.8 Hz, 1 H), 8.01-7.98 (m, 2 H), 7.56 (d, *J* = 8.4 Hz, 1 H), 7.35(s, 1 H), 3.54 (s, 2 H), 2.98 (q, *J* = 7.6 Hz, 2 H), 2.39 (br s, 4 H), 2.33 (br s, 4 H), 2.14 (s, 3 H), 1.31 (t, *J* = 7.6 Hz, 3 H). ^{13}C NMR (125 MHz, DMSO-d_6) δ 165.7, 150.1, 144.2, 141.7, 141.2, 140.8, 140.5, 133.3, 132.1, 131.8, 130.1 (q, *J* = 31.1 Hz), 129.9, 129.4, 125.1 (q, *J* = 270.6 Hz), 124.7, 121.6, 120.9, 119.7, 116.0, 109.9, 98.6, 80.2, 62.3, 55.6, 53.4, 46.6, 28.1, 15.4. HRMS (ESI) for $C_{30}H_{29}F_3N_6O$ $[M + H]^+$, calcd: 547.2428, Found: 547.2425. Purity 99.8% (t_R = 11.47 min).

4-Ethyl-3-(imidazo[1,2-*b*]pyridazin-3-ylethynyl)-*N*-(3-((4-methylpiperazin-1-yl)methyl)-5-(trifluoromethyl)phenyl)benzamide (5k).Compound **5k** was prepared by following a similar procedure as that of **5a**. Yield, 76%. ^{1}H NMR(400 MHz, DMSO-d_6) δ 10.58 (s, 1 H), 8.72 (dd, *J* = 4.4, 1.2 Hz, 1 H), 8.26 (dd, *J* =9.2 , 1.6 Hz, 1 H), 8.23 (m, 2 H), 8.20 (s, 1 H), 8.03 (s, 1 H), 7.99 (dd, *J* =8.0, 2.0 Hz, 1 H), 7.56 (d, *J* = 8.0 Hz, 1 H), 7.39 (q, *J* = 3.6 Hz, 1 H), 7.36 (s, 1 H), 3.55 (s, 2 H), 2.99 (q, *J* = 7.2 Hz, 2 H), 2.40 (br s, 4 H), 2.34 (br s, 4 H), 2.16 (s, 3 H), 1.31 (t, *J* = 7.2 Hz, 3 H). ^{13}C NMR (125 MHz, DMSO-d_6) δ 165.1, 149.8, 145.4, 141.1, 140.3, 140.1, 138.5, 132.7, 131.0, 129.6 (q, *J* = 31.2 Hz), 129.2, 129.0, 126.5, 124.6 (q, *J* = 270.7 Hz), 124.2, 121.5,

120.4, 119.4, 115.5, 112.2, 96.6, 81.1, 61.9, 55.1, 52.9, 46.1, 27.6, 15.0. HRMS (ESI) for $C_{30}H_{29}F_3N_6O$ $[M + H]^+$, calcd: 547.2428, Found: 547.2424. Purity 99.5% (tR = 23.41 min).

***N*-(4-ethyl-3-(imidazo[1,2-*a*]pyridin-3-ylethynyl)phenyl)-3-((4-methylpiperazin-1-yl) methyl)-5-(trifluoromethyl)benzamide(5l).** Compound **5l** was prepared by following a similar procedure as that of **5a**. Yield, 83%. ^{1}H NMR(400 MHz, DMSO-d_6) δ 10.57 (s, 1 H), 8.59 (d, J = 6.4 Hz, 1 H), 8.28 (s, 1 H), 8.20 (s, 1 H), 8.07 (s,1 H), 8.03 (s, 1 H), 7.97 (d, J = 8.0 Hz, 1 H), 7.75 (d, J = 8.8 Hz, 1 H), 7.55 (d, J = 8.0 Hz, 1 H), 7.46 (t, J = 7.2 Hz, 1 H), 7.36 (s, 1 H), 7.20 (t, J = 6.8 Hz, 1 H), 3.54 (s, 2 H), 2.98 (q, J = 7.6 Hz, 2 H), 2.40 (br s, 4 H), 2.34 (br s, 4 H), 2.15 (s, 3 H), 1.32 (t, J = 7.6 Hz, 3 H). ^{13}C NMR (125 MHz, DMSO-d_6) δ 165.3, 149.2, 145.8, 141.2, 140.3, 138.9, 132.8, 131.2, 129.6 (q, J = 31.0 Hz), 128.9, 127.0, 125.9, 124.6 (q, J = 270.6 Hz), 124.2, 121.7, 120.4, 1128.0, 115.5, 114.5, 108.0, 97.4, 81.2, 61.8, 55.1, 52.9, 46.1, 27.1, 14.9. HRMS (ESI) for $C_{31}H_{30}F_3N_5O$ $[M + H]^+$, calcd: 546.2475, Found: 547.2465. Purity 99.6% (t_R = 16.56 min).

3-(Imidazo[1,2-*a*]pyrazin-3-ylethynyl)-4-methyl-*N*-(3-((4-methylpiperazin-1-yl)methyl)-5-(trifluoromethyl)phenyl)benzamide (5m). Compound **5m** was prepared by following a similar procedure as that of **9**. Yield, 82%.^{1}H NMR(400 MHz, DMSO-d_6) δ 10.59 (s, 1 H), 9.22 (d, J = 1.2 Hz, 1 H), 8.68 (dd, J = 4.8, 1.6 Hz, 1 H), 8.32 (d, J = 1.6 Hz, 1 H), 8.28 (s, 1 H), 8.20 (s, 1 H), 8.14 (d, J = 4.4 Hz, 1 H), 8.03 (s, 1 H), 7.97 (dd, J = 8.0, 1.6 Hz, 1 H), 7.57 (d, J = 8.0 Hz, 1 H), 7.36 (s, 1 H), 3.55 (s, 2 H), 2.63 (s, 3 H), 2.40 (br s, 4 H), 2.35 (br s, 4 H), 2.16 (s, 3 H). ^{13}C NMR (125 MHz, DMSO-d_6) δ 165.6, 144.3, 144.1, 141.6, 141.2, 140.8, 140.4, 133.2, 131.7, 131.6, 130.9, 130.1(d, J = 31.4 Hz), 129.6, 125.1 (d, J = 270.4 Hz), 124.7, 122.3, 120.9, 119.8, 116.0, 109.9, 98.9, 80.6, 62.3, 55.5, 53.4, 46.5, 21.4. HRMS (ESI) for $C_{29}H_{25f3}N_6O$ $[M + H]^+$, calcd: 533.2271, Found: 533.2275. Purity 95.4% (t_R = 7.78 min).

3-(Imidazo[1,2-*a*]pyrazin-3-ylethynyl)-4-isopropyl-*N*-(3-((4-methylpiperazin-1-yl)methyl)-5-(trifluoromethyl)phenyl)benzamide (5n). Compound **5n**was prepared by following a similar procedure as that of **9**. Yield, 80%. ^{1}H NMR(400 MHz, DMSO-d_6) δ 10.60 (s, 1 H), 9.22 (s, 1 H), 8.64 (d, J = 4.0 Hz, 1 H), 8.32 (s, 1 H), 8.28 (s, 1 H), 8.20 (s, 1 H), 8.15 (d, J = 4.0 Hz, 1 H), 8.02 (s, 2 H), 7.62 (d, J = 8.0 Hz, 1 H), 7.36 (s, 1 H), 3.61-3.56 (m, 1 H), 3.54 (s, 2 H), 2.39 (br s, 4 H), 2.33 (br s, 4 H), 2.15 (s, 3 H), 1.34 (d, J = 6.8 Hz, 6 H). ^{13}C NMR (125 MHz, DMSO-d_6) δ 165.2, 153.8, 143.7, 141.2, 140.7, 140.3, 140.0, 132.8, 131.8, 131.3, 129.6 (q, J = 31.0 Hz), 129.5, 126.1, 124.6 (q, J = 270.9 Hz), 124.2, 120.7, 120.4, 119.3, 115.5, 109.4, 98.1, 79.9, 61.8, 55.1, 52.9, 46.1, 32.0, 23.2. HRMS (ESI) for $C_{31}H_{31}F_3N_6O$ $[M + H]^+$, calcd: 561.2584, Found: 561.2580. Purity 99.4% (t_R = 14.87 min).

4-Cyclopropyl-3-(imidazo[1,2-a]pyrazin-3-ylethynyl)-N-(3-((4-methylpiperazin-1-yl)methyl)-5-(trifluoromethyl)phenyl)benzamide (5o). Compound **5o** was prepared by following a similar procedure as that of **9**. Yield, 85%. ^{1}H NMR(400 MHz, DMSO-d_6) δ 10.56 (s, 1 H), 9.21 (d, J = 1.2 Hz, 1 H), 8.68-8.66 (m, 1 H), 8.31 (d, J = 1.6 Hz, 1 H), 8.28 (s, 1 H), 8.19 (s, 1 H), 8.14 (d, J = 4.8 Hz, 1 H), 8.02 (s, 1 H), 7.96-7.94 (m, 1 H), 7.35 (s, 1 H), 7.15 (d, J = 8.4 Hz, 1 H), 3.54 (s, 2 H), 2.56-2.53 (m, 1 H), 2.40 (br s, 4 H), 2.34 (br s, 4 H), 2.15 (s, 3 H), 1.23-1.17 (m, 2 H), 0.93-0.89 (m, 2 H). ^{13}C NMR (125 MHz, DMSO-d_6) δ 165.6, 150.2, 144.1, 141.6, 141.2, 140.8, 140.5, 132.5, 131.9, 131.7, 130.1 (q, J = 31.1 Hz), 129.9, 125.1 (q, J = 270.8 Hz), 124.7, 124.5, 122.2, 120.9, 119.9, 116.0, 110.0, 99.1, 80.3, 62.3, 55.6, 53.4, 46.6, 15.0, 11.1. HRMS (ESI) for $C_{31}H_{29}F_3N_6O$ $[M + H]^+$, calcd: 559.2428, Found: 559.2427. Purity 98.2% (t_R = 14.51 min).

4-(*tert*-Butyl)-3-(imidazo[1,2-*a*]pyrazin-3-ylethynyl)-*N*-(3-((4-methylpiperazin-1-yl)methyl)-5-(trifluoromethyl)phenyl)benzamide (5p).

Compound **5p**was prepared by following a similar procedure as that of **9**. Yield, 85%.^{1}H NMR(400 MHz, DMSO-d_6) δ 10.62 (s, 1 H), 9.23 (d, J = 1.2 Hz, 1 H), 8.66-8.65 (m, 1 H),8.36 (d, J = 2.0 Hz, 1 H), 8.27 (s, 1 H), 8.21 (s, 1 H), 8.16 (d, J = 4.4 Hz, 1 H), 8.03 (s, 1 H), 8.01-7.98 (s, 1 H),7.66 (d, J = 8.8 Hz, 1 H), 7.37 (s, 1 H), 3.56 (s, 2 H), 2.42 (br s, 4 H), 2.34 (br s, 4 H), 2.16 (s, 3 H), 1.61 (s, 9 H). ^{13}C NMR (125 MHz, DMSO-d_6) δ 165.6, 155.4, 144.3, 141.7, 141.2, 140.8, 140.3, 135.0, 133.3, 131.8, 130.2 (q, J = 31.4 Hz), 129.7, 127.1, 125.1 (q, J = 270.9 Hz), 124.7, 121.0, 120.7, 119.8, 116.0, 110.1, 101.3, 82.5, 62.3, 55.6, 53.4, 46.6, 36.8, 30.7. HRMS (ESI) for $C_{32}H_{33}F_3N_6O$ $[M + H]^+$, calcd: 575.2741, Found: 575.2735. Purity 99.1% (t_R = 15.84 min).

3-(Imidazo[1,2-*b*]pyridazin-3-ylethynyl)-4-isopropyl-*N*-(3-((4-methylpiperazin-1-yl)methyl)-5-(trifluoromethyl)phenyl)benzamide (5q).

Compound **5q** was prepared by following a similar procedure as that of **9**. Yield, 81%. ^{1}H NMR(400 MHz, DMSO-d_6) δ 10.59 (s, 1 H), 8.73-8.71 (m, 1 H), 8.27-8.19 (m, 4 H), 8.02-8.00 (m, 2 H), 7.61 (d, J = 8.4 Hz, 1 H), 7.40-7.35 (m, 2 H),3.66-3.59 (m, 1 H), 3.56 (s, 2 H), 2.40 (br s, 4 H), 2.33 (br s, 4 H), 2.15 (s, 3 H), 1.33 (d, J = 6.8 Hz, 6 H). ^{13}C NMR (125 MHz, DMSO-d_6) δ 165.6, 154.5, 146.0, 141.7, 140.8, 140.5, 139.1, 133.2, 131.7, 130.1 (d, J = 31.4 Hz), 129.9, 127.0, 126.7, 125.1 (q, J = 270.9 Hz), 124.7, 121.6, 120.9, 120.0, 116.0, 112.7, 97.1, 81.8, 62.3, 55.6, 53.4, 46.6, 32.3, 23.6. HRMS (ESI) for $C_{31}H_{31}F_3N_6O$ $[M + H]^+$, calcd: 561.2584, Found: 561.2579. Purity 99.1% (t_R = 28.98 min).

3-(Imidazo[1,2-*a*]pyridin-3-ylethynyl)-4-isopropyl-*N*-(3-((4-methylpiperazin-1-yl)methyl)-5-(trifluoromethyl)phenyl)benzamide(5r).

Compound **5r** was prepared by following a similar procedure as that of **9**. Yield, 80%. ^{1}H NMR(400 MHz, DMSO-d_6) δ 10.58 (s, 1 H), 8.58 (d, J = 6.8 Hz, 1 H), 8.28 (d, J = 2.0 Hz, 1 H),

8.20 (s, 1 H), 8.07 (s, 1 H), 8.02 (s, 1 H), 8.00-7.98 (m, 1 H), 7.75 (d, J = 9.2 Hz, 1 H), 7.60 (d, J = 8.4 Hz, 1 H), 7.48-7.44 (m, 1 H), 7.36 (s, 1 H), 7.22-7.19 (m, 1 H), 3.61-3.56 (m, 1 H), 3.55 (s, 2 H), 2.40 (br s, 4 H), 2.34 (br s, 4 H), 2.16 (s, 3 H), 1.35 (d, J = 6.8 Hz, 6 H). ^{13}C NMR (125 MHz, DMSO-d_6) δ 165.8, 153.9, 146.3, 141.7, 140.8, 139.4, 133.3, 131.9, 130.1 (q, J = 31.4 Hz), 129.6, 127.5, 126.5, 126.4, 125.1 (q, J = 270.7 Hz), 124.7, 121.8, 120.9, 118.5, 116.0, 115.0, 108.5, 97.9, 81.9, 62.3, 55.6, 53.4, 46.6, 32.5, 23.6. HRMS (ESI) for $C_{32}H_{32}F_3N_5O$ $[M + H]^+$, calcd: 560.2632, Found: 560.2628. Purity 99.6% (t_R = 17.89 min).

Methyl 4-ethyl-3-iodobenzoate(7a).[24]

To a suspension of methyl 3-amino-4-ethylbenzoate (10 g, 55.8 mmol) in water (100 mL) was added conc. H_2SO_4 (10 mL) at 0 ^oC and then a solution of $NaNO_2$ (4.6 g, 67 mmol) in water (50 ml) was added dropwise. After the mixture has been stirred at 0 ^oC for 2 hours, a solution of KI (10.2 g, 61.4 mmol) in water (50 ml) was added dropwise and the mixture was warmed to rt slowly. The reaction was quenched with saturated $Na_2S_2O_3$ solution and was extracted with ethyl acetate. The organic layer was washed with brine, dried over Na_2SO_4, concentrated in vacuo and further purified by flash chromatography on silica gel to give the title compound **7a** (11.3 g, 70% yield).^{1}H NMR (400 MHz, $CDCl_3$) δ 8.44 (d, J = 1.6 Hz, 1 H), 7.92-7.90 (m, 1 H), 7.24 (d, J = 2.8 Hz, 1 H), 3.87 (s, 3 H), 2.75 (q, J = 7.6 Hz, 2 H), 1.19 (t, J = 7.6 Hz, 3 H).

Methyl 3-iodo-4-methylbenzoate (7m). [24]

Compound **7m** was prepared by following a similar procedure as that of **7a**. Yield, 68%. ^{1}H NMR (400 MHz, DMSO-d_6) δ 8.46 (s, 1 H), 7.89 (dd, J = 8.0, 1.2 Hz, 1 H), 7.29 (d, J = 8.0 Hz, 1 H), 3.90 (s, 3 H), 2.47 (s, 3 H).

Methyl 3-iodo-4-isopropylbenzoate (7n). Compound **7n** was prepared by following a similar procedure as that of **7a**. Yield, 50%. ^{1}H NMR (400 MHz, DMSO-d_6) δ 8.33 (d, J = 2.0 Hz, 1 H),

7.93 (dd, *J* = 8.0, 2.0 Hz, 1 H), 7.47 (d, *J* = 8.0 Hz, 1 H), 3.84 (s, 3 H), 3.20-3.10 (m, 1 H), 1.20 (d, *J* = 6.8 Hz, 6 H). MS (ESI) m/z 305 $[M + H]^+$.

Methyl 4-cyclopropyl-3-iodobenzoate (7o). Compound**7o** was prepared by following a similar procedure as that of **7a**. Yield, 63%. ^{1}H NMR (400 MHz, DMSO-d_6) δ 8.32 (d, *J* = 2.0 Hz, 1 H), 7.86-7.83 (m, 1 H), 7.05 (d, *J* = 8.0 Hz, 1 H), 3.83 (s, 3 H), 2.09-2.03 (m, 1 H), 1.11-1.06 (m, 2 H), 0.76-0.72 (m, 2 H). MS (ESI) m/z 303 $[M + H]^+$.

Methyl 4-(*tert*-butyl)-3-iodobenzoate (7p). Compound **7p** was prepared by following a similar procedure as that of **7a**. Yield, 40%.^{1}H NMR(400 MHz, DMSO-d_6) δ 8.47 (d, *J* = 1.2 Hz, 1 H), 7.91-7.89 (m, 1 H), 7.59 (d, *J* = 8.4 Hz, 1 H), 3.84 (s, 3 H), 1.51 (s, 9 H). MS (ESI) m/z 319 [M + H]$^+$.

Methyl 4-ethyl-3-ethynylbenzoate (8a). [24]

To a solution of methyl 4-ethyl-3-iodobenzoate (11.3 g, 39 mmol) in CH_3CN (100 mL) was added$PdCl_2(PPh_3)_2$ (548 mg, 0.78 mmol), CuI (149 mg, 0.78 mmol) and Et_3N (16 ml, 117 mmol). The mixture was filled with Ar and stirred at 60^{o}C overnight. The reaction mixture was filtered through a pad of Celite and concentrated under vacuum. The residue was redissolved in MeOH (100 mL) and K_2CO_3 (16 g, 117 mmol) was added. The mixture was added at rt for 1 hour.The reaction mixture was filtered through a pad of Celite and concentrated under vacuum. The resulting residue was purified by silica gel column to give the title compound **8a** (6.6 g, 90% yield). ^{1}H NMR (400 MHz, $CDCl_3$) δ 8.13 (s, 1H), 7.95-7.92 (m, 1 H), 7.29-7.26 (m, 1 H), 3.90 (s, 3 H), 3.28 (s, 1 H), 2.86 (q, *J* = 7.6 Hz, 2 H), 1.25 (t, *J* = 7.6 Hz, 3 H).

Methyl 3-ethynyl-4-methylbenzoate (8m). [24]Compound **8m** was prepared by following a similar procedure as that of **8a**. Yield, 92%.^{1}H NMR (400 MHz, DMSO-d_6) δ 7.93 (d, *J* = 1.2 Hz, 1 H), 7.85 (dd, *J* = 8.0, 1.6 Hz, 1 H), 7.44 (d, *J* = 8.4 Hz, 1 H), 4.49 (s, 1 H), 3.84 (s, 3 H), 2.44 (s,

3 H).

Methyl 3-ethynyl-4-isopropylbenzoate (8n). Compound **8n** was prepared by following a similar procedure as that of **8a**. Yield, 89%. ^{1}H NMR (400 MHz, DMSO-d_6) δ 7.94-7.91 (m, 2 H), 7.51 (d, J = 8.0 Hz, 1 H), 4.49 (s, 1 H), 3.84 (s, 3 H), 3.45-3.39 (m, 1 H), 1.22 (d, J = 6.8 Hz, 6 H). MS (ESI) m/z 203 $[M + H]^+$.

Methyl 4-cyclopropyl-3-ethynylbenzoate (8o). Compound **8o** was prepared by following a similar procedure as that of **8a**. Yield, 88%. ^{1}H NMR (400 MHz, DMSO-d_6) δ 7.92 (s, 1 H), 7.82 (d, J = 8.0 Hz, 1 H), 6.99 (d, J = 8.4 Hz, 1 H), 4.49 (s, 1 H), 3.84 (s, 3 H), 2.42-2.35 (m, 1 H), 1.13-1.11 (m, 2 H), 0.83-0.81 (m, 2 H). MS (ESI) m/z 201 $[M + H]^+$.

Methyl 4-(*tert*-butyl)-3-ethynylbenzoate(8p). Compound **8p** was prepared by following a similar procedure as that of **8a**. Yield, 88%. ^{1}H NMR (400 MHz, DMSO-d_6) δ 7.97 (m, 1 H), 7.88 (d, J = 8.0 Hz, 1 H), 7.54 (d, J = 8.4 Hz, 1 H), 4.64 (s, 1 H), 3.84 (s, 3 H), 1.48 (s, 9 H). MS (ESI) m/z 217 $[M + H]^+$.

4-Ethyl-3-ethynyl-*N*-(3-((4-methylpiperazin-1-yl)methyl)-5-(trifluoromethyl)phenyl)benza mide (9).

To a solution of methyl 4-ethyl-3-ethynylbenzoate (6.6 g, 35.1 mmol) and 3-((4-methylpiperazin-1-yl)methyl)-5-(trifluoromethyl)aniline (9.1 g, 33.3 mmol) in THF (80 mL) was added t-BuOK (5.9 g, 52.6 mmol) at -20 ^{o}C. The mixture was warmed to rt slowly. After completion of the reaction, the mixture was poured into ice-water and extracted with ethyl acetate. The organic layer was washed with brine, dried over Na_2SO_4, concentrated in vacuo and purified by flash chromatography on silica gel to give the title compound **9** (13.1 g, 92% yield). ^{1}H NMR (400 MHz, DMSO-d_6) δ 10.52 (s, 1 H), 8.17 (s, 1 H), 8.10 (d, J = 2.0 Hz, 1 H), 8.00 (s, 1 H), 7.95-7.93 (m, 1 H), 7.48 (d, J = 8.4 Hz, 1 H), 7.35 (s, 1 H), 4.50 (s, 1 H), 3.54 (s, 2 H),

2.83 (q, *J* = 7.6 Hz, 2 H), 2.40-2.33 (m, 8 H), 2.16 (s, 3 H), 1.22 (d, *J* = 7.2 Hz, 3 H). MS (ESI) m/z 430 $[M + H]^+$.

Methyl 3-(imidazo[1,2-a]pyrazin-3-ylethynyl)-4-methylbenzoate (10m)

Compound **10m** was prepared by following a similar procedure as that of **5a**. Yield, 91%.^{1}H NMR (400 MHz, DMSO-d_6) δ 9.20 (s, 1 H), 8.72 (d, *J* = 4.4 Hz, 1 H), 8.27 (s, 1 H), 8.21 (s, 1 H), 8.12 (d, *J* = 4.4 Hz, 1 H), 7.92 (dd, *J* = 8.0, 1.2 Hz, 1 H), 7.54 (d, *J* = 8.0 Hz, 1 H),3.88 (s, 3 H), 2.60 (s, 3 H). MS (ESI) m/z 292 $[M + H]^+$.

Methyl 3-(imidazo[1,2-*a*]pyrazin-3-ylethynyl)-4-isopropylbenzoate (10n).Compound **10n** was prepared by following a similar procedure as that of **5a**. Yield, 68%. ^{1}H NMR (400 MHz, $CDCl_3$) δ 9.16 (s, 1 H), 8.26 (d, *J* = 4.4 Hz, 1 H), 8.24 (s, 1 H), 8.07 (d, *J* = 4.4 Hz, 1 H), 8.05-8.02 (m, 2 H), 7.44 (d, *J* = 8.0 Hz, 1 H), 3.94 (s, 3 H), 3.63-3.52 (m, 1 H), 1.36 (d, *J* = 6.4 Hz, 6 H). MS (ESI) m/z 320 $[M + H]^+$.

Methyl 4-cyclopropyl-3-(imidazo[1,2-a]pyrazin-3-ylethynyl)benzoate(10o). Compound **10o** was prepared by following a similar procedure as that of **5a**. Yield, 82%.^{1}H NMR(400 MHz, DMSO-d_6) δ 9.19 (s, 1 H), 8.70 (d, *J* = 4.0 Hz, 1 H), 8.26 (s, 1 H), 8.19 (s, 1 H), 8.11 (d, *J* = 4.0 Hz, 1 H), 7.88 (d, *J* = 8.4 Hz, 1 H), 7.10 (d, *J* = 8.4 Hz, 1 H), 3.86 (s, 3 H), 1.21-1.19 (m, 2 H), 0.88-0.85 (m, 2 H). MS (ESI) m/z 318 $[M + H]^+$.

Methyl 4-(*tert*-butyl)-3-(imidazo[1,2-*a*]pyrazin-3-ylethynyl)benzoate (10p). Compound **10p** was prepared by following a similar procedure as that of **5a**. Yield, 64%.^{1}H NMR (400 MHz, DMSO-d_6) δ 9.21 (s, 1 H), 8.65 (d, *J* = 4.0 Hz, 1 H), 8.26-8.25 (m, 2 H), 8.15 (s, 1 H), 7.96-7.94 (m, 1 H), 7.63 (d, *J* = 8.4 Hz, 1 H), 3.89 (s, 3 H), 1.57 (s, 9 H). MS (ESI) m/z 334 $[M + H]^+$.

Methyl 3-(imidazo[1,2-b]pyridazin-3-ylethynyl)-4-isopropylbenzoate (10q). Compound **10q** was prepared by following a similar procedure as that of **5a**. Yield, 73%. ^{1}H NMR (400 MHz,

$CDCl_3$) δ 8.49-8.47 (m, 1 H), 8.27 (d, *J* = 2.0 Hz, 1 H), 8.05-8.02 (m, 2 H), 8.00-7.98 (m, 1 H), 7.40 (d, *J* = 8.0 Hz, 1 H), 7.15-7.11 (m, 1 H), 3.92 (s, 3 H), 3.71-3.64 (m, 1 H), 1.35 (d, *J* = 6.8 Hz, 6 H). MS (ESI) m/z 320 $[M + H]^+$.

Methyl 3-(imidazo[1,2-*a*]pyridin-3-ylethynyl)-4-isopropylbenzoate (10r).

Compound **10r** was prepared by following a similar procedure as that of **5a**. Yield, 71%.^{1}H NMR (400 MHz, DMSO-d_6) δ 8.66 (s, 1 H), 8.17 (s, 1 H), 7.95 (d, *J* = 8.4 Hz, 1 H), 7.76 (br s, 1 H), 7.57 (d, *J* = 8.0 Hz, 1 H), 7.50-7.43 (m, 2 H), 7.19 (t, *J* = 6.8 Hz, 1 H), 3.87 (s, 3 H), 3.58-3.51 (m, 1 H), 1.32 (t, *J* = 7.2 Hz, 6 H). MS (ESI) m/z 319 $[M + H]^+$.

Cells and Treatment. MPMs were prepared and cultured from C57BL/6 mice using the method described in our previous paper.[30] MPMs were incubated in DMEM media (Gibco) supplemented with 10% FBS, 100 U/mL penicillin, and 100 mg/mL streptomycin at 37 °C with 5% CO_2. Compounds were added into cell cultural medium in DMSO solution with the final concentration of DMSO is 0.1‰.

Reagents. LPS was purchased from Sigma Chemical Co. (St. Louis, MO, USA). Mouse TNF-α and IL-6 ELISA kits were purchased from eBiosscience (San Diego, CA, USA). Anti-CD68 was from Santa Cruz Biotechnology (Santa Cruz, CA, USA). Trizol-reagent and primers were purchased from Invitrogen (Invitrogen, Carlsbad, CA, USA).

***In Vitro* Kinase Assay.** The functional assays of compounds on the kinase activities of Abl were determined using the FRET-based *Z′*-Lyte assay system according to the manufacturer's instructions (Invitrogen, USA). Tyrosine 2 peptide was used as Abl substrate. The reactions were carried out in 384-well plates in a 10 μL of reaction volume with appropriate amount of kinases in 50 mM HEPES (pH 7.5), 10 mM $MgCl_2$, 1.0 mM EGTA, and 0.01% Brij-35. The reactions were incubated 1 h at room temperature in the presence of 2.0 μM of substrate with 10 mM of

ATP and in the presence of various concentrations of the compounds. The development reagent was then added for further 2 h room temperature incubation followed by the addition of stop solution. Fluorescence signal ratio of 445 nm (Coumarin)/520 nm (fluorescin) was examined on EnVision Multilabel Reader (Perkin-Elmer, Inc.).

The effects of compounds on the kinases DDR1 and DDR2 were assessed by using a LanthaScreen Eu kinase activity assay technology (Invitrogen, USA). Kinase reactions are performed in a 10 μL volume in low-volume 384-well plates. The kinases in reaction buffer consists of 50 mM HEPES pH 7.5, 0.01% BRIJ-35, 10 mM MgCl2, and 1 mM EGTA, the concentration of Fluorescein-Poly GAT substrate (Invitrogen, USA) in the assay is 100 nM. Kinase reactions were initiated with the addition of 100 nM ATP in the presence of serials of dilutions of compounds. The reactions were allowed to proceed for 1 h at room temperature before a 10 μL preparation of EDTA (20 mM) and Eu-labeled antibody (4 nM) in TR-FRET dilution buffer are added. The final concentration of antibody in the assay well is 2 nM, and the final concentration of EDTA is 10 mM. The plate is allowed to incubate at room temperature for one more hour before the TR-FRET emission ratios of 665 nm/340 nm were acquired on a PerkinElmer EnVision multilabel reader (Perkin-Elmer, Inc.). Data analysis and curve fitting were performed using GraphPad Prism4 software.

Active-Site Dependent Competition Binding Assay−Kinomescan Screening. The binding affinity of **5n** with DDR1 was analyzed by KINOME scan system conducted by Ambit Bioscience (San Diego, USA). Briefly, kinases were tagged with DNA. The ligands were biotinylated and immobilized to streptavidin-coated beads. The binding reactions were assembled by incubating DNA-tagged kinases, immobilized ligands, and test compounds in binding reactions (20% SeaBlock, 0.17 × PBS, 0.05% tween-20, 6 mM DTT) for 1.0 h at room

temperature. The affinity beads were washed with washing buffer (1× PBS, 0.05% Tween-20) first and then elution buffer (1× PBS, 0.05% Tween 20, 0.5 μM nonbiotinylated affinity ligands). The kinase concentration in the eluate was determined by quantitative PCR of the DNA tagged to the kinase. The ability of the test compound to bind to the kinase was evaluated with percent control (%) as (test compound signal − positive control signal)/negative control signal – positive control signal) × 100%. Negative control is DMSO control (100% ctrl) and positive control is control compound (0% ctrl).

Immunoprecipitation and Western Blot Analysis. Primary human lung fibroblast was cultured in Medium199 (Sigma Aldrich) containing 10% fetal bovine serum (FBS) and maintained at 37 °Cin a humidified incubator with 5% CO_2 and 95% air. Cells were cultured in 100 mm tissue culture dishes in complete media (M199 with 10% FBS) until they reached a high density (~80% confluence). Then cells were starved for 4 hours in M199 with 1% FBS. After that cells were cultured in 5mL of complete media with 50 μg/mL collagen and indicated concentration of **5n** for 24 hours. Collagen and collagen with DMSO were added as controls. Cells were lysed, supernatants were recovered by centrifugation at 13,000 rpm, protein concentration was measured and equal amounts of total protein were separated by SDS-PAGE. For immunoprecipitation, lysates were pre-cleared with protein A/G beads (Thermo Fisher Scientific). We used 200 μg cellular protein in 1 ml lysis buffer per immunoprecipitation reaction. To each sample, 1 μg of DDR2 (Cell Signaling #12133) antibody was added with 50 μl protein A/G bead slurry; each sample was then allowed to rotate overnight at 4°C on a nutator. Immunoprecipitated complexes were washed twice in lysis buffer, boiled in sample buffer, and subjected to SDS-PAGE. Proteins were transferred to PVDF membranes (Bio-Rad; Hercules, CA) followed by blockade for 1 hour in 5% bovine serum albumin in TBS-T. Membranes were

incubated overnight at 4 °C with primary antibody phospho-DDR1 (Tyr792, Cell Signaling #11994), DDR1 (Santa Cruz SC-532), DDR2 (Cell Signaling #12133), phospho-Tyrosine (Millipore, 4G10), anti-c-ABL (Santa Cruz sc-23), anti-p-c-ABL (Santa Cruz sc-293130) and TUBULIN ALPHA (Biorad, MCA77D800). Membranes were incubated with corresponding HRP-conjugated secondary antibody (Pierce Biotechnologies; Rockford, IL) for 1 hour. Specific bands were detected using the enhanced chemiluminescence reagent (ECL, Perkin Elmer Life Sciences; Boston, MA) on antoradiographic film.

Crystallization and Structure Determination. The kinase domain of human DDR1 (Uniprot Q08345, residues 601-913) was expressed as an N-terminal 6xHis fusion in Sf9 cells and purified by Nickel affinity chromatography, followed by tag cleavage with TEV protease and then size exclusion chromatography on an S200 column (GE Healthcare). Protein at 13.6 mg/ml in 50 mM HEPES, 300 mM NaCl, 0.5 mM TCEP, 2% DMSO was incubated with 1 mM compound **5n** for 4 hours on ice, and then filtered to 0.22 μm. 150 nL sitting drops were set up with the highest resolution crystals being obtained from a 1:2 ratio of protein to mother liquor (10% ethylene glycol, 0.2 M sodium sulfate, 24% PEG3350, 0.1 M bis-tris-propane pH 7.1). Crystals were cryoprotected in mother liquor supplemented with 20% ethylene glycol and vitrified in liquid nitrogen. Diffraction was carried out at Diamond Light Source beamline I03 at 100K. Data were indexed and integrated using XDS [31, 32] and scaled using AIMLESS.[33] Phases were identified using molecular replacement in PHASER.[34] Structures were built using PHENIX.AUTOBUILD[35] and then refined and modified using PHENIX.REFINE[36] and COOT.[35] The refined structure was validated with MolProbity[36] and the atomic coordinate files deposited in the Protein Data Bank with Autodep.[37]

Determination of Pharmacokinetic Parameters in Rats. Male SD rats, weighing 180-220g

(Southern China Medical University, China) were utilized for the studies. The protocol was approved by the Animal Care and Use Committee, GIBH. Animals were maintained on standard animal chow and water ad libitum, in a climate controlled room (23±1 ^{o}C, 30–70% relative humidity, a minimum of 10 exchanges of room air per hour and a 12-h light/dark cycle) for one week prior to experiments. The compound was dissolved in the solution containing 2%DMSO, 4%ethanol, 4%castor oil and 90%ddH_2O. Pharmacokinetic properties of SD rats (male) were determined following i.v. and oral administration. Animals were randomly distributed into two experimental groups (n = 3). The oral groups were given 25 mg/kg by gastric gavage. The other group was dosed by injection into the tail vein (5mg/kg). After single administration, whole blood samples (100-200 μL) were obtained from the orbital venous plexus at the following time points after dosing: 5,10, 30 min and 1, 2, 3, 4, 6, 8,11 and 24 h (p.o.); 2,10, 30 min and 1, 2, 3, 4, 6, 8, 11 and 24 h (i.v.).Whole blood samples were collected in heparinized tubes. The plasma fraction was immediately separated by centrifugation (8,000 rpm, 6 min, 4 °C) and stored at −20 °C until LC-MS analysis.The rats were humanely euthanasia by carbon dioxide 24 hours after experiment without pain. The pharmacokinetics parameters were calculated by analyzing the compound concentration in plasma samples using the pharmacokinetic software DAS.2.0.

Animals. Male C57BL/6 mice (6–8 weeks age) were obtained from the Animal Center of Wenzhou Medical University (Wenzhou, China). Animal experiments were performed in accordance with the Guide for the Care and Use of Laboratory Animals. All animal experimental procedures were approved by the Wenzhou Medical University Animal Policy and Welfare Committee.

Acute Toxicity Assay. Male C57BL/6 mice weighing 18-20 g were randomly divided into three groups (n = 5 per group). Mice were gavaged administration with 200 μL of drug (at 200 mg/kg

or 400 mg/kg in physiological saline). Mice in control group received 200 μL of physiological saline. After the drug i.g., body weight changes were recorded for 7 days.

LPS-induced ALI. Male C57BL/6 mice were randomly divided into four groups, designated "CON" (8 mice, only received the vehicle of 0.9% saline), "LPS" (8 mice, received 5 mg/kg LPS alone), "LPS+20 mg/kg BID **5n**" (8 mice, received both compound **5n**at 20 mg/kg and 5 mg/kg LPS), and "LPS+40 mg/kg BID **5n**" (8 mice, received both compound **5n**at 40 mg/kg and 5 mg/kg LPS). Prior to intratracheal injection of LPS, the mice were treated orally two times per day with **5n** at the dosages of 20 mg/kg and 40 mg/kg continuously for one week. Mice were then euthanized with ketamine 6 h after LPS induction. The blood was collected and the chest cavity of each animal was carefully opened, and the collection of BALF and lung tissues were performed.

BALF Analysis. The collected BALF was centrifuged at 1000 rpm for 10 min at 4 °C, the supernatant was used for protein concentration detection and subsequent cytokine determinations. The precipitation was resuspended using 50 μL physiological saline. The total number of cells on BALF was detected by cell counting instrument. The number of neutrophils on BALF was examined using Wright-Gimesa stain.

Determination of TNF-α and IL-6. The pro-inflammatory cytokines TNF-α and IL-6 in cell culture, BALF and serum were determined with an ELISA kit according to the manufacturer's instructions. The total amount of the inflammatory factor in the culture media was normalized to the total protein quantity of the viable cell pellets.

Real-time Quantitative PCR (RT-qPCR). Lung tissues were homogenized in TRIZOL reagent for extraction of RNA according to each manufacturer's protocol. Both reverse transcription and quantitative PCR were carried out using a two-step M-MLV Platinum SYBR Green

qPCRSuperMix-UDG kit (Invitrogen, Carlsbad, CA). EppendorfMastercyclereprealplex detection system (Eppendorf, Hamburg, Germany) was used for RT-qPCR analysis. The primers of genes including TNF-α, IL-6, IL-1β, IL-12, ICAM-1, VCAM-1, and β-actin were obtained from Invitrogen. The amount of each gene was determined and normalized to the amount of β-actin.

Lung Wet/dry Weight Ratio. The right upper lobe of lung was excised. After removal of the excessive water on the tissue surface, the wet weight was recorded. The sample was then dried at 60 °C for 48 h until no weight change to record the dry weight. The wet weight/dry weight ratio (W/D) was calculated and used as an index of lung edema.

Pulmonary Histopathology and Immunohistochemistry Analysis. The right lower lobe of lung was excised and fixed with 4% formalin. The lung tissues were embedded with paraffin, sliced to 5 μm sections, and stained with hematoxylin and eosin (HE). Mice lung histopathology images were acquired using a microscope (Nikon Model Eclipse 80i, Nikon, Tokyo, Japan). The immunohistochemistry analysis was performed following the anti-CD68 antibody staining protocol.

Statistical Analysis. All *in vitro* experiments were assayed in triplicate. Data are expressed as means ± SD. All statistical analyses were performed using GraphPad Pro. Prism 6.0 (GraphPad, SanDiego, CA). Student's t-test was employed to analyze the differences between sets of data. A p value < 0.05 was considered statistically significant.

Computational Study. All the procedure was performed in Maestro 11.2 (version 11.2, Schrödinger, LLC, New York, NY, 2017). The 3D structure of DDR2 structure has not been determined to date, while many homologous structures with high sequence identity have been reported. We chose the crystal structure of human DDR1 (PDB ID 3ZOS), which shares 57%

sequence identity with DDR2, as a template to generate a homology model for the active form of DDR2. The homology model of the DDR2 was built by Prime Homology Modeling, and all the parameters were default.

The DDR2 protein was processed using the "Protein Preparation Wizard" workflow in Maestro 9.4 (version 11.2, Schrödinger, LLC, New York, NY, 2017) to add bond orders and hydrogens. All hetatm residues and crystal water molecules beyond 5 Å from het group were removed. Compounds **5a**, **5b**, **5i** and **5j** were built by in LigPrep module using OPLS-2005 force field. Glide module was used as docking program. The grid-enclosing box was placed on the centroid of the 0LI, which was extracted from the crystal structure of DDR1. Standard precision (SP) approach of Glide was adopted to dock compounds **5a**, **5b**, **5i**, and **5j** to DDR2 with the default parameters.

ASSOCIATED CONTENT

Supporting Information

The results of sequence alignment of DDR1and DDR2, the selectivity profiling study of compound **5n**, crystallization and structure determination of DDR1-**5n**, PK profiles of **5n**, *in vivo* acute study of **5n**, the ^{1}H and ^{13}C NMR spectra of compounds **5a**-**5r**, HPLC traces for the representative compounds, and Molecular Formula Strings. This material is available free of charge via the Internet at http://pubs.acs.org.

AUTHOR INFORMATION

Corresponding Author

*For G.L.: E-mail, wzmcliangguang@163.com.

*For K.D.: E-mail, dingke@jnu.edu.cn

*For X.L.: E-mail, luxy2016@jnu.edu.cn.phone, +86-20-85221523

Author Contributions

[#]Zhen Wang, Yali Zhang and Daniel Pinkas contributed equally to this work.

Notes

The authors declare no competing financial interest.

ACKNOWLEDGMENT

The authors appreciate the financial support from National Natural Science Foundation of China (21572230, 81673285 and 81425021), Guangdong Province (2014TQ01R341, 2015A030306042, 2015A030312014, 2016A050502041 and Nanyue-Baijie Award) and Jinan University. We thank Diamond Light Source for beamtime (proposal mx15433), as well as the staff of beamline I03 for assistance with data collection. The SGC is a registered charity (number 1097737) that receives funds from AbbVie, Bayer Pharma AG, Boehringer Ingelheim, Canada Foundation for Innovation, Eshelman Institute for Innovation, Genome Canada, Innovative Medicines Initiative (EU/EFPIA) [ULTRA-DD grant no. 115766], Janssen, Merck KGaA Darmstadt Germany, MSD, Novartis Pharma AG, Ontario Ministry of Economic Development and Innovation, Pfizer, São Paulo Research Foundation-FAPESP, Takeda, and Wellcome [106169/ZZ14/Z].

ABBREVIATIONS

LPS, lipopolysaccharide; IL-6, interleukin-6; MIP-1α,macrophage inflammatory protein-1α; MPMs, mouse primary peritoneal macrophages; ALI, mouse acute lung injure; DDRs, discoidin domain receptors; RTKs, transmembrane receptor tyrosine kinases; MCP-1,monocyte chemoattractant protein-1; TNF-α,tumor necrosis factor-α; INF-γ, interferon-γ; IC_{50}, half-

maximal (50%)inhibitory concentration of a substance; ATP, adenosine triphosphate; K_d, binding constant; Abl, abelson murine leukemia viral oncogene; EPHA7, Ephrin type-A receptor 7; EPHB2, Ephrin type-B receptor 2; LCK, lymphocyte-specific protein tyrosine kinase; LOK, serine/threonine kinase 10; TIE2, angiopoietin-1 receptor; TrkA, nerve growth factor receptor A; ELISA, enzyme linked immunosorbent assays; BID, twice daily; W/D, Wet/Dry; BALF, bronchial alveolar lavage fluid; ICAM-1, intercellular cell adhesion molecule-1; VCAM-1, vascular cell adhesion molecule 1.

REFERENCES

(1) Valiathan, R. R.; Marco, M.; Leitinger, B.; Kleer, C. G.; Fridman,R. Discoidin domain receptor tyrosine kinases: new players in cancerprogression. *Cancer Metastasis Rev.***2012**, *31*, 295−321.

(2) Leitinger, B. Discoidin domain receptor functions in physiologicaland pathological conditions. *Int. Rev. Cell Mol. Biol.***2014**, *310*, 39−87.

(3) Iwai, L. K.; Luczynski, M. T.; Huang, P. H. Discoidin domainreceptors: a proteomic portrait. *Cell. Mol. Life Sci.***2014**, *71*, 3269−3279.

(4) Borza, C. M.; Pozzi, A. Discoidin domain receptors in disease.*Matrix Biol.***2014**, *34*, 185−192.

(5) Kothiwale, S.; Borza, C. M.; Lowe, E. W., Jr.; Pozzi, A.; Meiler, J.Discoidin domain receptor 1 (DDR1) kinase as target for structurebased drug discovery. *Drug Discov. Today***2015**, *20*, 255−261.

(6) Ju, G. X.; Hu, Y. B.; Du, M. R.; Jiang, J. L. Discoidin domainreceptors (DDRs): potential implications in atherosclerosis. *Eur. J. Pharmacol.***2015**, *751*, 28−33.

(7) Li, Y.; Lu, X.; Ren, X.; Ding, K. Small molecule discoidindomain receptor kinase inhibitors and potential medical applications. *J. Med. Chem.***2015**, *58*, 3287−3301.

(8) Matsuyama, W.; Wang, L.; Farrar, W. L.; Faure, M.; Yoshimura, T. Activation of discoidin domain receptor 1 isoform b with collagen up-regulates chemokine production in human macrophages: role of p38 mitogen-activated protein kinase and NF-kappa B. *J. Immunol.***2004**, *172*, 2332 − 2340.

(9) Flamant, M.; Placier, S.; Rodenas, A.; Curat, C. A.; Vogel, W. F.; Chatziantoniou, C.; Dussaule, J. C. Discoidin domain receptor 1 null mice are protected against hypertension-induced renal disease. *J. Am. Soc. Nephrol.***2006**, *17*, 3374 − 3381.

(10) Avivi-Green, C.; Singal, M.; Vogel, W. F. Discoidin domain receptor 1-deficient mice are resistant to bleomycin-induced lung fibrosis. *Am. J. Respir. Crit. Care Med.* **2006**, *174*, 420−427.

(11) Wang, Z.; Bian, H.; Bartual, S. G.; Du, W.; Luo, J.; Zhao, H.; Zhang, S.; Mo, C.; Zhou, Y.; Xu, Y.; Tu, Z.; Ren, X.; Lu, X.; Brekken, R. A.; Yao, L.; Bullock, A. N.; Su, J.; Ding, K. Structure-based design of tetrahydroisoquinoline-7-carboxamides as selective discoidin domain receptor 1 (DDR1) inhibitors. *J. Med. Chem.***2016**, *59*, 5911 − 5916.

(12) Wang, Z.; Zhang, Y.; Bartual, S. G.; Luo, J.; Xu, T.; Du, W.; Xun, Q.; Tu, Z.; Brekken, R. A.; Ren. X.; Bullock, A. N.; Liang, G.; Lu, X.; Ding, K. Tetrahydroisoquinoline-7-carboxamide derivatives as new selective discoidin domain receptor 1 (DDR1) inhibitors. *ACS Med. Chem. Lett.***2017**, *8*, 327 - 332.

(13) Poudel, B.; Yoon, D. S.; Lee, J. H.; Lee, Y. M.; Kim, D. K. Collagen I enhances functional activities of human monocyte-derived dendritic cells via discoidin domain receptor 2. *Cell Immunol.***2012**, *278*, 95 - 102.

(14) Poudel, B.; Ki, H. H.; Lee, Y. M.; Kim, D. K. Induction of IL-12 production by the activation of discoidin domain receptor 2 via NF-kappaB and JNK pathway. *Biochem. Biophys. Res. Commun.***2013**, *434*, 584 - 588.

(15) Yang J, Wheeler SE, Velikoff M, Kleaveland KR, Lafemina MJ, Frank JA, Chapman HA, Christensen PJ, Kim KK. Activated alveolar epithelial cells initiate fibrosis through secretion of mesenchymal proteins. *Am J Pathol.***2013**, *183*, 1559–1570.

(16) Luo, Z.; Liu, H.; Sun, X.; Guo, R.; Cui, R.; Ma, X.; Yan, M. RNA interference against discoidin domain receptor 2 ameliorates alcoholic liver disease in rats. *PLoS One***2013**, *8*, e55860.

(17) Olaso, E.; Ikeda, K.; Eng, F. J.; Xu, L.; Wang, L. H.; Lin, H. C.; Friedman, S. L.; DDR2 receptor promotes MMP-2-mediated proliferation and invasion by hepatic stellate cells. *J. Clin. Invest.***2001**, *108*, 1369–1378.

(18) Ruiz, P. A.; Jarai, G. Collagen I induces discoidin domain receptor (DDR) 1 expression through DDR2 and a JAK2-ERK1/2-mediated mechanism in primary human lung fibroblasts. *J. Biol. Chem.***2011**, *286*, 12912 - 12923.

(19) Richters, A.; Nguyen, H. D.; Phan, T.; Simard, J. R.; Grutter, C.; Engel, J.; Rauh, D. Identification of type II and III DDR2 inhibitors. *J. Med. Chem.***2014**, *57*, 4252−4262.

(20) Murray, C. W.; Berdini, V.; Buck, I. M.; Carr, M. E.; Cleasby, A.; Coyle, J. E.; Curry, J. E.; Day, J. E.; Day, P. J.; Hearn, K.; Iqbal, A.; Lee, L. Y.; Martins, V.; Mortenson, P. N.; Munck, J. M.; Page, L. W.; Patel, S.; Roomans, S.; Smith, K.; Tamanini, E.; Saxty, G. Fragment-based discovery of potent and selective DDR1/2 Inhibitors. *ACS Med. Chem. Lett.***2015**, *6*, 798 − 803.

(21) Terai, H.; Tan, L.; Beauchamp, E. M.; Hatcher, J. M.; Liu, Q.; Meyerson, M.; Gray, N. S.; Hammerman, P. S. Characterization of DDR2 inhibitors for the treatment of DDR2 mutated non-small cell lung cancer. *ACS Chem. Biol.***2015**, *10*, 2687-2696.

(22) Day, E.; Waters, B.; Spiegel, K.; Alnadaf, T.; Manley, P. W.; Buchdunger, E.; Walker, C.; Jarai, G. Inhibition of collagen-induced discoidin domain receptor 1 and 2 activation by imatinib, nilotinib and dasatinib. *Eur. J. Pharmacol.***2008**, *599*, 44 –53.

(23) Sonogashira, K. Development of Pd-Cu catalyzed cross-coupling of terminal acetylenes with sp2-carbon halides. *J. Organomet. Chem.***2002**, *653*, 46–49.

(24) Gao, M.; Duan, L.; Luo, J.; Zhang, L.; Lu, X.; Zhang, Y.; Zhang, Z.; Tu, Z.; Xu, Y.; Ren, X.; Ding, K. Discovery and optimization of 3-(2-(Pyrazolo[1,5-a]pyrimidin-6-yl)ethynyl)benzamidesas novel selective and orally bioavailable discoidin domain receptor 1 (DDR1) inhibitors. *J. Med. Chem.***2013**, *56*, 3281 − 3295.

(25)Chang, S.; Zhang, L.; Xu, S.; Luo, J.; Lu, X.; Zhang, Z.; Xu,T.; Liu, Y.; Tu, Z.; Xu, Y.; Ren, X.; Geng, M.; Ding, J.; Pei, D.; Ding, K.Design, synthesis, and biological evaluation of novel conformationallyconstrained inhibitors targeting epidermal growth factorreceptor threonine790 →methionine790 mutant. *J. Med. Chem*.**2012**, *55*, 2711−2723.

(26) Li, Y.; Shen, M.; Zhang, Z.; Luo, J.; Pan, X.; Lu, X.; Long, H.; Wen, D.; Zhang, F.; Leng, F.; Li, Y.; Tu, Z.; Ren, X.; Ding, K. Design, synthesis, and biological evaluation of 3-(1H-1,2,3-triazol-1-yl)benzamide derivatives as potent pan Bcr-Abl inhibitors including the threonine(315)->isoleucine(315) mutant. *J. Med. Chem.***2012**, *55*, 10033 – 10046.

(27) Fabian, M. A.; Biggs, W. H., 3rd; Treiber, D. K.; Atteridge, C. E.; Azimioara, M. D.; Benedetti, M. G.; Carter, T. A.; Ciceri, P.; Edeen, P. T.; Floyd, M.; Ford, J. M.; Galvin, M.; Gerlach, J. L.; Grotzfeld, R. M.; Herrgard, S.; Insko, D. E.; Insko, M. A.; Lai, A. G.; Lelias, J. M.; Mehta, S. A.; Milanov, Z. V.; Velasco, A. M.; Wodicka, L. M.; Patel, H. K.; Zarrinkar, P. P.; Lockhart, D. J. A small molecule-kinase interaction map for clinical kinase inhibitors. *Nat. Biotechnol.***2005**, *23*, 329−336.

(28) Belkina, N. V.; Liu, Y.; Hao, J. J.; Karasuyama, H.; Shaw, S. LOK is a major ERM kinase in resting lymphocytes and regulates cytoskeletal rearrangement through ERM phosphorylation. *Proc. Natl. Acad. Sci. USA* **2009**, *106*, 4707–4712.

(29) Sasahira, T.; Ueda, N.;Kurihara, M.; Matsushima, S;Ohmori, H.;Fujii, K.;Bhawal, UK.; Yamamoto, K.;Kirita, T.;Kuniyasu, H. Tropomyosin receptor kinases B and C are tumor progressive and metastatic marker in colorectal carcinoma. *Hum. Pathol.* **2013**, *44*, 1098–1106.

(30) Chen, G.; Zhang, Y.; Liu, X.; Fang, Q.; Wang, Z.; Fu, L.; Liu, Z.; Wang, Y.; Zhao, Y.; Li, X.; Liang, G. Discovery of a new inhibitor of myeloid differentiation 2 from cinnamamide derivatives with antiinflammatory activity in sepsis and acute lung injury. *J. Med. Chem.***2016**, *59*, 2436 − 2451.

(31) Kabsch, W. XDS. *Acta Crystallogr. D Biol. Crystallogr.* **2010,** *66*, 125−132.

(32) Leslie, A. G. W.; Powell, H. R. Processing diffraction data with MOSFLM. *Evolv. Methods Macro. Crystallogr.* **2007,** *245*, 41-51.

(33) Evans, P. R.; Murshudov, G. N. How good are my data and what is the resolution? *Acta Crystallogr. D Biol. Crystallogr.* **2013,** *69*, 1204-1214.

(34) McCoy, A. J.; Grosse-Kunstleve, R. W.; Adams, P. D.; Winn, M. D.; Storoni, L. C.; Read, R. J. Phaser crystallographic software. *J. Appl. Crystallogr.* **2007,** *40*, 658-674.

(35) Adams, P. D.; Afonine, P. V.; Bunkoczi, G.; Chen, V. B.; Davis, I. W.; Echols, N.; Headd, J. J.; Hung, L. W.; Kapral, G. J.; Grosse-Kunstleve, R. W.; McCoy, A. J.; Moriarty, N. W.; Oeffner, R.; Read, R. J.; Richardson, D. C.; Richardson, J. S.; Terwilliger, T. C.; Zwart, P. H. PHENIX: a comprehensive Python-based system for macromolecular structure solution. *Acta Crystallogr. D Biol. Crystallogr.* **2010,** 66, 213-221.

(36) Chen, V. B.; Arendall, W. B., 3rd; Headd, J. J.; Keedy, D. A.; Immormino, R. M.; Kapral, G. J.; Murray, L. W.; Richardson, J. S.; Richardson, D. C. MolProbity: all-atom structure validation for macromolecular crystallography. *Acta Crystallogr. D Biol. Crystallogr.* **2010,** *66*, 12-21.

(37) Yang, H.; Guranovic, V.; Dutta, S.; Feng, Z.; Berman, H. M.; Westbrook, J. D. Automated and accurate deposition of structures solved by X-ray diffraction to the Protein Data Bank. *Acta Crystallogr. D Biol Crystallogr.* **2004,** *60*, 1833-1839

Table of Contents graphic